Functional analysis of *Arabidopsis* LBP/BPI related-1 and -2 in lipopolysaccharide-induced plant defense responses

（LPS に対する防御応答における
シロイヌナズナ LBP/BPI 関連タンパク質-1 と-2 の機能解析）

Sayaka Iizasa

2018

Dedication

This thesis work is dedicated to my husband Ei'ichi.
Thank you for your steadfast love, support, encouragement,
and undying belief to me.

Acknowledgements

I would like to acknowledge my foremost, respected teacher, Assoc. Prof. Dr. Yukio Nagano of Saga University for his long-standing supports, enthusiastic teaching, and transcendental knowledge. I am also grateful to Prof. Dr. Keiichi Watanabe, Prof. Dr. Kenji Fukudome, Assoc. Prof. Dr. Susumu Mitsutake, and Assoc. Prof. Dr. Toshihisa Ueda of Saga University and Assoc. Prof. Dr. Toshiharu Yasaka of Kagoshima University for their kindly support and helpful discussion, which forward and highly promoted this work. I would also like to thank Dr. Cyril Zipfel of The Sainsbury Laboratory and Assoc. Prof. Dr. Takehito Inaba of Miyazaki University for their kindly providing *Arabidopsis* seeds and helpful comments.

In addition, special thanks to Prof. Dr. Hisanori Tamaki of Kagoshima University for his long-standing supports and encourages. I want also to thank my lab members for their valuable help in the experiments.

This work was supported by the Foundation for Research Fellowships of the Japan Society for the Promotion of Science for Young Scientists (DC1) to S. I. (21· 86) and by Research grant for advanced research, United Graduate School of Agricultural Sciences, Kagoshima University.

Table of contents

List of abbreviations

ABA: abscisic acid
AtLBR-1: *Arabidopsis* LBP/BPI related-1
AtLBR-1N: recombinant protein of AtLBR-1 containing 215 N-terminal residues
AtLBR-2: *Arabidopsis* LBP/BPI related-2
AtLBR-2N: recombinant protein of AtLBR-2 containing 214 N-terminal residues
atlbr-DKO: *atlbr-1/-2-1* double mutant
BP: biological process
BPI: bactericidal/permeability-increasing protein
CBB: coomassie brilliant blue
CC: cellular component
eLPS: prepared LPS from *Escherichia coli*
ET: ethylene
FDR: false discovery rate
Flg22: active epitope of bacterial flagellin
fls2: FLAGELLIN-SENSITIVE 2 mutant
GO: gene ontology
IB: immunoblotting
JA: jasmonic acid
LBP: LPS-binding protein
Log_2FC: log fold change
LPS: lipopolysaccharide
NPR1: *NON-EXPRESSOR OF PR1*
MF: molecular function
PAMP: pathogen-associated molecular pattern
pLPS: commercial LPS from *Pseudomonas aeruginosa*
PLUNC: palate, lung, and nasal epithelial clone
PR1: *pathogenesis-related 1*
qRT-PCR: quantitative RT-PCR
RNA-Seq: mRNA sequencing
ROS: reactive oxygen species
SA: salicylic acid
SAG: conjugated SA glucoside
sfGFP: super folder GFP
TX-100: Triton X-100

Abstract

Lipopolysaccharide (LPS), a major constituent of the outer membrane of Gram-negative bacteria, acts as a pathogen-associated molecular pattern for both animals and plants. LPS-binding protein (LBP) and bactericidal/permeability-increasing protein (BPI), which bind to LPS and play important roles in immunity of mammals, have been well studied. However, the molecule contributing to LPS binding in plants is mostly unknown. The *Arabidopsis* genome carries two genes encoding LBP/BPI-related proteins which I designated as AtLBP/BPI related-1 (AtLBR-1) and AtLBP/BPI related-2 (AtLBR-2). I found that their N-terminal domains were co-purified with cell wall derived LPS when expressed in *E. coli*. Since this finding implied the direct binding of AtLBRs to LPS, I also confirmed binding by using LPS-free AtLBRs and purified LPS. AtLBRs directly bind to both rough and smooth types of LPS. I also demonstrated that LPS-treated *atlbr* mutant *Arabidopsis* exhibit a significant delay of induction of defence-related gene *pathogenesis-related 1* (*PR1*) but no other *PR* genes. Furthermore, LPS-treated *atlbr* mutants showed defects in reactive oxygen species (ROS) generation. These results demonstrate that, as well as LBP and BPI of mammals, AtLBRs also play an important role in the LPS-induced immune response of plants.

AtLBR-2, in particular, located in apoplastic region, which is an important place for

plant–pathogen interactions, and exhibited a high LPS-binding affinity. I investigated the role of AtLBR-2 in more detail by comprehensive transcriptomic analysis using mRNA sequencing (RNA-Seq) technology. RNA-Seq data analysis revealed that LPS treatment significantly altered the expression of 2,139 genes, with 605 up-regulated and 1,534 down-regulated genes in WT. Comparative analysis of differentially expressed genes between WT and *atlbr-2* mutant revealed that 65 genes were identified as a AtLBR-2-dependent up-regualted genes. Gene ontology (GO) analysis demonstrated the importance of these 65 genes for the enrichment of some defense-related GO terms, including responses to bacterium, wounding, drug, abscisic acid stimulus, and salicylic acid (SA) stimulus. In fact, among of these 65 genes, 14 genes, including *PR1*, are known to be induced by SA. Therefore, I investigated whether LPS-induced SA accumulation levels were altered in *atlbr-2* mutants. I found that the accumulation levels of conjugated SA glucoside (SAG) between WT and the *atlbr-2* showed significant differences at 8 h after LPS treatment. Furthermore, I observed the up-regulation of *PR1* in the SA-treated *atlbr-2* to be at the same level, as or more, than that of WT plants. These results suggested the existence of an SA (SAG)-mediated LPS signaling system via AtLBR-2. AtLBR-2 might be a key molecule that is indispensable for the up-regulation of defense-related genes and for SA signaling pathway This study is the first to demonstrate the importance of AtLBRs in LPS-induced plant defense responses.

Chapter 1:

Characterization of *Arabidopsis* LBP/BPI related-1 and -2 in LPS-induced plant defense responses

Introduction

Plants detect pathogen invasions by recognition of pathogen-associated molecular patterns (PAMPs). PAMP perception induces various defense responses. Lipopolysaccharide (LPS), a primary constituent of the outer membrane of Gram-negative bacteria, is one of the most studied PAMPs. LPS causes defense responses such as generation of nitrogen oxide (NO) and reactive oxygen species (ROS) in *Arabidopsis*, tobacco, and rice suspension cells [1–3]. LPS also induces expression of *pathogenesis-related* (*PR*) genes, which are up-regulated in pathological or stressful situations, in *Arabidopsis* leaves [1]. In addition, LPS induces stomatal closure and NO production in guard cells [3]. Further, investigation of the LPS recognition mechanism is at the forefront in plant innate immunity studies. Recently, Ranf *et al.* identified that the bulb-type lectin S-domain-1 receptor-like kinase LORE (lipooligosaccharide-specific reduced elicitation) is required for sensing of LPS from *Pseudomonas* and *Xanthomonas* species [4]. However, it is still unclear which molecule(s),

including LORE, can directly bind to LPS. Thus, the identification of these molecule(s) will enhance our understanding of the overall LPS recognition system.

In mammals, there are two well-studied proteins that directly bind to LPS, LPS-binding protein (LBP) and bactericidal/permeability-increasing protein (BPI). Human LBP (hLBP) and human BPI (hBPI) structurally resemble each other with 45% amino acid sequence identity. Both proteins play important roles in the regulation of defense responses against LPS. Mammalian LPS recognition is orchestrated by several LPS binding proteins, including LBP, BPI, and a membrane protein CD14, which transfers LPS to a mammalian LPS receptor complex TLR4/MD-2 [5, 6]. LBP, a serum glycoprotein produced principally by hepatocytes, is critical to rapid and effective signal transduction for induction of proinflammatory cytokines, because it facilitates the transfer of LPS to CD14, then to TLR4/MD-2. In addition, BPI, which is a glycoprotein purified from granules of neutrophils, also binds to LPS with higher affinity than LBP [5]. The binding of BPI to LPS increases the permeability of the bacterial membranes and opsonizes bacteria to enhance phagocytosis by neutrophils [5]. Another important aspect of BPI is the attenuation of the LPS-induced inflammatory response by competitive inhibition against LBP [5].

LBP and BPI belong to a protein family called the LBP/BPI/PLUNC (palate, lung, and nasal epithelial clone) superfamily [7]. PLUNC protein, an abundant secretory product in

human nasal lavage fluid, also can bind to LPS and has been shown to suppress the growth of bacteria [8, 9]. Interestingly, LBP/BPI/PLUNC superfamily proteins have been identified in various species including chicken, fish, and oyster [10–15]. This superfamily can be divided into two subfamilies; LBP/BPI and PLUNC. Ovocalyxin-36 (OCX-36) is an abundant eggshell protein of chicken which is related to the PLUNC subfamily. OCX-36 binds to LPS and shows inhibitory activity against growth of Staphylococcus aureus [16]. LBP/BPI subfamily proteins of oyster Crassostrea gigas (Cg-BPI1 and Cg-BPI2) also display LPS binding and bactericidal activities [15, 17]. Expression of LBP/BPI subfamily genes was induced by bacterial challenge or LPS treatment in various fish such as rainbow trout, Atlantic cod, carp, and ayu [11–14]. However, LBP/BPI/PLUNC superfamily proteins have not been characterised in plants. The fact that members of both subfamilies (i.e., hLBP, hBPI, OCX-36 and Cg-BPI) bind to LPS and participate in innate immune responses against potential bacterial invasion motivated the current study to characterize plant proteins belonging to the LBP/BPI/PLUNC superfamily.

In Chapter 1, I characterized two genes of *Arabidopsis*, AtLBP/BPI related-1 (AtLBR-1) and AtLBP/BPI related-2 (AtLBR-2), which belong to the LBP/BPI subfamily rather than the PLUNC subfamily. Because many LBP/BPI/PLUNC superfamily proteins were characterized by their LPS binding ability, I studied whether AtLBRs can bind to LPS.

As the results, the recombinant N-terminal domain of AtLBRs is found to bind to LPS directly. In addition, LPS-treated *atlbr* mutants showed the defect in immune responses, such as *PR1* gene expression and ROS production. Altogether, these results demonstrate the biological importance of LBRs for induction of LPS-triggered defense responses in plants and the functional similarities among LBP/BPI subfamily from various organisms.

Results

Identification of LBP/BPI-related proteins in *Arabidopsis* genome.

To identify putative LBP/BPI-related genes in *Arabidopsis*, a BLAST search was performed using the hLBP amino acid sequence as a query against the *Arabidopsis* genome sequence. As a result, two candidates were found. I termed these proteins AtLBR-1 (*At1g04970*) and AtLBR-2 (*At3g20270*). AtLBR-1 and AtLBR-2 consist of 488 and 477 amino acids including signal sequences, respectively. Putative mature proteins of AtLBR-1 and AtLBR-2 have calculated molecular masses of 50.7 kDa and 49.8 kDa, respectively. They share 41% amino acid sequence identity to each other. Both proteins display 42–46% similarity and 23–25% identity to the amino acids of hLBP and hBPI, respectively.

A multiple alignment of LBP/BPI proteins showed that the residues determining backbone flexibility (Gly) or rigidity (Pro) are highly conserved (Fig. 1-1). In BPI, two apolar

binding pockets, located in each N- and C-terminal domain, are thought to play a role in binding of LPS acyl chains [18]. The hydrophobic residues constituting the apolar binding pockets are also highly conserved in both AtLBR-1 and AtLBR-2 (Fig. 1-1). In contrast, a pair of cysteine residues, which form an intramolecular disulphide bond in hBPI [18], is not found in the AtLBR N-terminal domains.

Phylogenetic trees were constructed using the maximum-likelihood method with amino acid sequences of AtLBR proteins and members of the LBP/BPI/PLUNC superfamily (Fig. 1-2). The tree was divided into two major branches, LBP/BPI and PLUNC, as shown previously [7]. AtLBRs were clearly classified as a LBP/BPI subfamily. Plant members of the LBP/BPI subfamily are clustered together and are clearly distinct from the animal sub-branch of LBP/BPI subfamily. Although AtLBRs have sequences related to LBP/BPI proteins of animals, they evolved independently from animal ones.

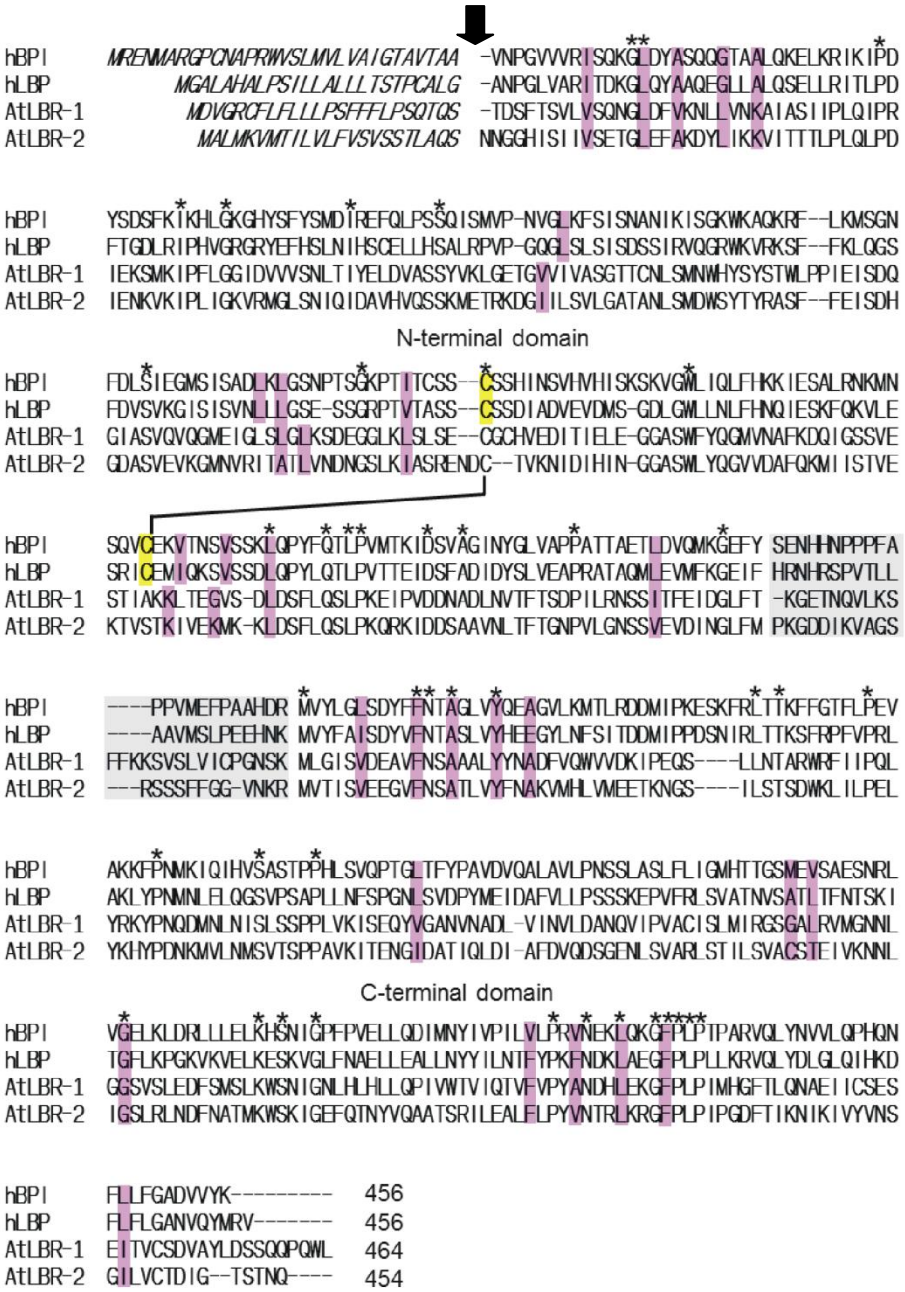

Figure 1-1. Sequence homologies of AtLBRs.

Multiple alignment of hBPI, hLBP, AtLBR-1, and AtLBR-2. Alignment was performed with Clustal-W. Amino acid numbers refer to the mature proteins. Conserved residues are indicated by asterisks. An arrow indicates the putative cleavage site by the signal peptidase. Conserved cysteines forming the single disulphide bond in hBPI [18] are highlighted in yellow. The residues constituting the apolar binding pockets are highlighted in pink. Proline-rich central domains characterized for hBPI as well as the corresponding sequences in hLBP and AtLBRs are highlighted in grey.

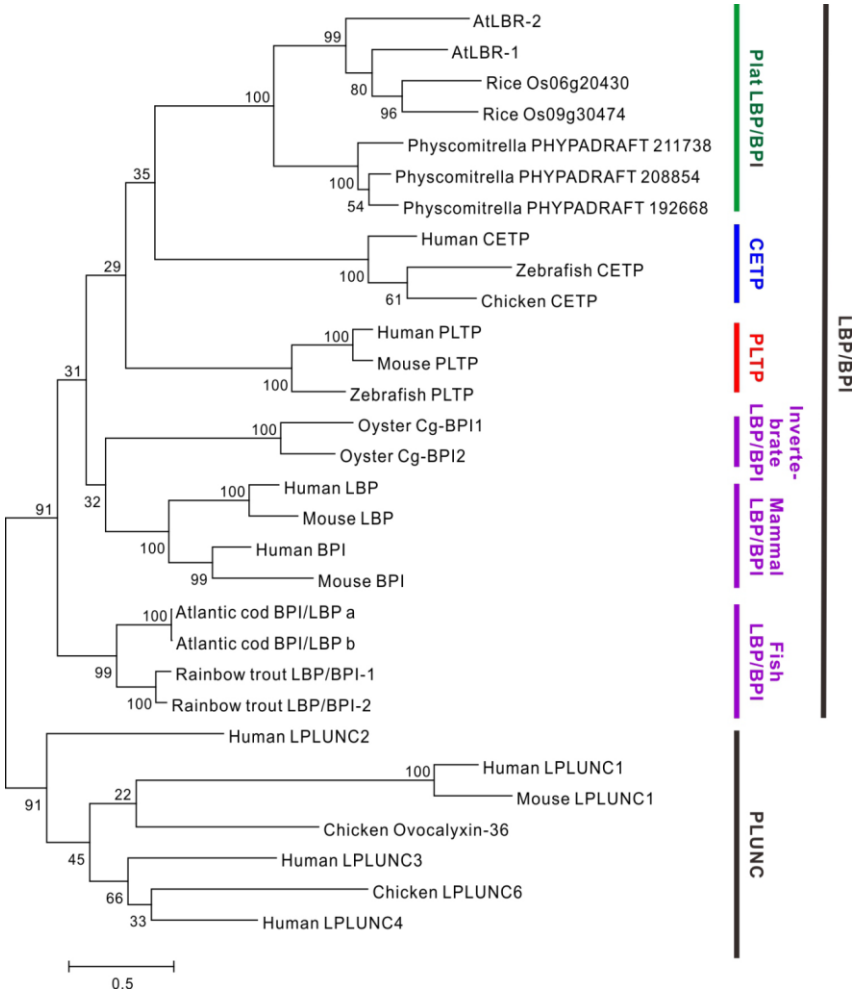

Figure 1-2. Phylogenetic analysis of AtLBRs.

Phylogenetic analysis of the LBP/BPI/PLUNC superfamily. The phylogenetic tree was generated by the maximum-likelihood method using MEGA6.06. Bootstrap values (%) were estimated by 1000 replications and are presented at each branch point. Protein sequences were downloaded from NCBI: AtLBR-1 (NM_100375), AtLBR-2 (NM_112918), human CETP (NM_000078), chicken CETP (NM_001034814), zebrafish CETP (BC085584), human PLTP (NM_006227), mouse PLTP (BC003782), zebrafish PLTP (NM_001003519), Cg-BPI1 (FJ669301), Cg-BPI2 (HM992925), human LBP (M35533), mouse LBP (NM_008489), human BPI (DQ414688), mouse BPI (NM_177850), Atlantic cod LBP/BPI a (AY102628), Atlantic cod LBP/BPI b (AY102629), rainbow trout LBP/BPI-1 (NM_001124585), rainbow trout LBP/BPI-2 (NM_001124198), human LPLUNC1 (NM_033197), human LPLUNC2 (NM_025227), human LPLUNC3 (NM_182658), human LPLUNC4 (NM_182519), mouse LPLUNC1 (NM_001012392), chicken LPLUNC6 (XM_417463), and chicken ovocalyxin-36 (NM_001030861). Protein sequences were downloaded from Phytozome: Os09g30474 (LOC_Os09g30474), Os06g20430 (LOC_Os06g20430), *Physcomitrella* PHYPADRAFT 211738 (Pp1s73_8V6), *Physcomitrella* PHYPADRAFT 208854 (Pp1s49_176V6), and *Physcomitrella* PHYPADRAFT 192668 (Pp1s184_35V6).

Recombinant AtLBR-Ns were co-purified with LPS derived from expression host *Escherichia coli*.

Because it has been reported that the recombinant N-terminal domain of hLBP was co-purified with LPS derived from expression host *Escherichia coli* [19], I investigated if AtLBRs could be co-purified with LPS. I prepared a recombinant protein of AtLBR-1 containing 215 N-terminal residues (AtLBR-1N) and of AtLBR-2 containing 214 N-terminal residues (AtLBR-2N) as thioredoxin (Trx) and His-tag fusion protein. AtLBR-Ns were successfully expressed in *E. coli* and purified by Ni-affinity chromatography (Fig. 1-3A). A considerable amount of LPS was detected in the eluted fractions of both AtLBR-Ns; the elution pattern of LPS completely matched those of the recombinant proteins (Fig. 1-3B, top and middle panels, left side). In contrast, LPS was undetectable in the eluted fractions of the negative control Trx (Fig. 1-3B, bottom panel, left side). These results suggest that the AtLBR-Ns bind to LPS. In addition, LPS could be removed from AtLBR-Ns by Triton X-100 (TX-100) as previously reported in the hLBP study (Fig. 1-3B, right side) [19].

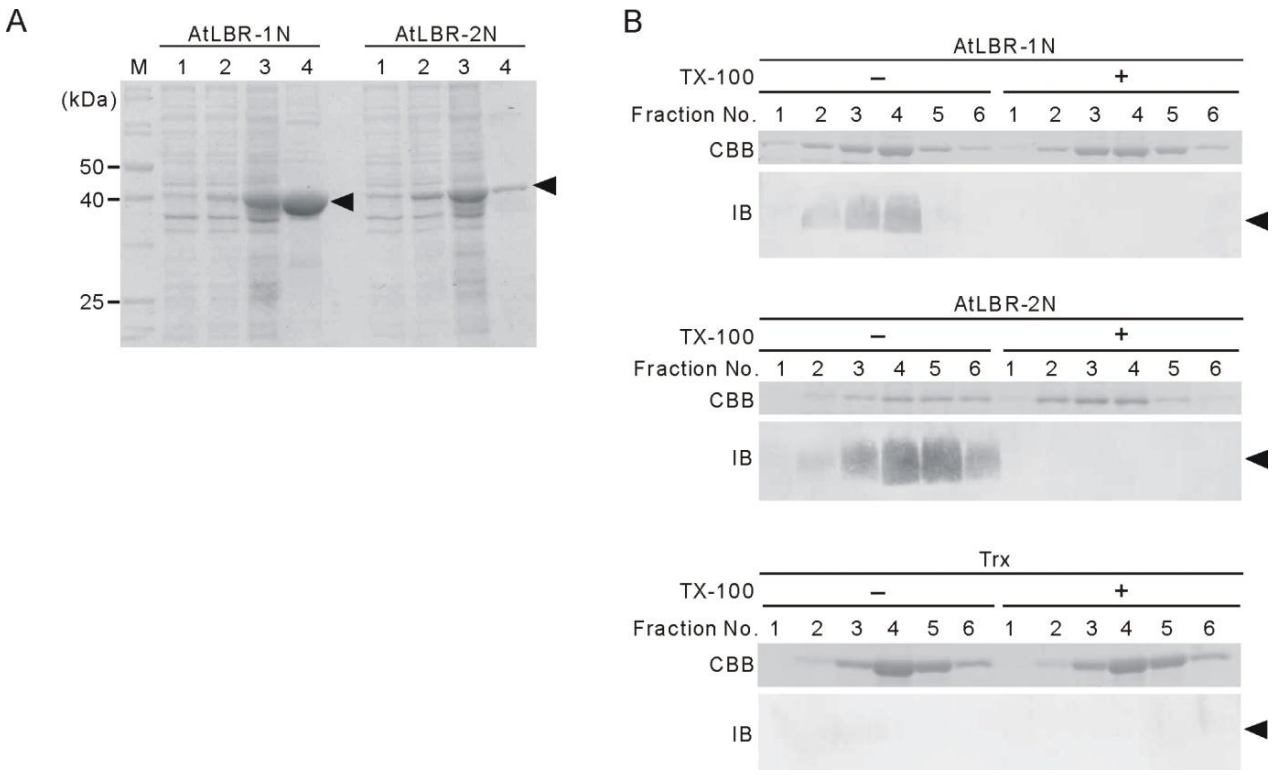

Figure 1-3. Co-purification of recombinant AtLBR-Ns with LPS.

(**A**) AtLBR-1N and AtLBR-2N were expressed in *E. coli* and purified by Ni-affinity chromatography (arrowhead). Lane 1: bacterial lysate before induction, Lane 2: bacterial lysate after IPTG-induction, Lane 3: soluble fractions, and Lane 4: purified fractions by Ni-affinity chromatography were analyzed by SDS-PAGE and CBB staining. (**B**) Recombinant AtLBR-Ns and control Trx were purified by Ni-affinity column in the absence or presence of 0.5% TX-100. Eluates were analyzed by SDS-PAGE (12% gel) followed by CBB staining (upper panels). LPS in the fractions were detected by immunoblotting (IB) (18% gel) using an anti-eLPS antibody (arrowhead, lower panels).

Recombinant AtLBR-Ns directly bind to purified LPS.

I examined whether AtLBR-Ns directly bind to purified LPS by using an LPS-binding assay reported previously [19]. LPS-free recombinant proteins were incubated with *E. coli* LPS (eLPS) and were trapped on a Ni-resin spin column. After washing, bound LPS was detected by immunoblotting (Fig. 1-4A). AtLBR-2N showed strong binding to eLPS, while eLPS binding to AtLBR-1N was relatively weak (Fig. 1-4A, lane 2, 5). These results demonstrate the direct binding between eLPS and AtLBR-Ns. Furthermore, the binding affinity of AtLBR-2N for eLPS seems higher than that of AtLBR-1N. In addition, I also examined whether AtLBRs bind to LPS from bacteria other than *E. coli*. *Pseudomonas aeruginosa* is an opportunistic bacterium found ubiquitously in the environment and infects many organisms from plants to humans [20, 21]. *P. aeruginosa* LPS (pLPS) induces NO bursts and ROS production in *Arabidopsis* suspension cells [1, 2]. Because the anti-LPS antibody cannot detect pLPS, I examined the binding of AtLBR-Ns to pLPS by a competition assay. A ten-fold amount of pLPS inhibited the binding of eLPS to AtLBR-Ns (Fig. 1-4A, lane 3, 6). These results show that AtLBRs interact with not only LPS from *E. coli* but also other Gram-negative bacteria such as *P. aeruginosa*.

Recombinant AtLBR-Ns bind to both smooth and rough LPS.

Gram-negative bacteria have either smooth or rough LPS. Smooth type LPS is composed of O-antigen repeats, a core oligosaccharide, and lipid A, while rough type LPS lacks the O-antigen repeats. Recombinant hLBP including the N-terminal domain binds equally well to both smooth and rough LPS [19]. Although hBPI also binds to both types of LPS directly, it has more potent bactericidal activity against bacteria containing rough type LPS [22, 23]. Therefore, I examined the binding ability of AtLBR-Ns to smooth and rough LPS. The anti-LPS antibody could detect both types of LPS at the same level (Fig. 1-4B, right panel). Like hLBP and hBPI, AtLBR-Ns also bound to both smooth and rough LPS (Fig. 1-4B). However, both AtLBR-Ns could bind to rough type LPS with higher affinity than to smooth type. Furthermore, the binding affinity of AtLBR-2N for both LPS seemed higher than that of AtLBR-1N, which is consistent with the above data (Fig. 1-4A).

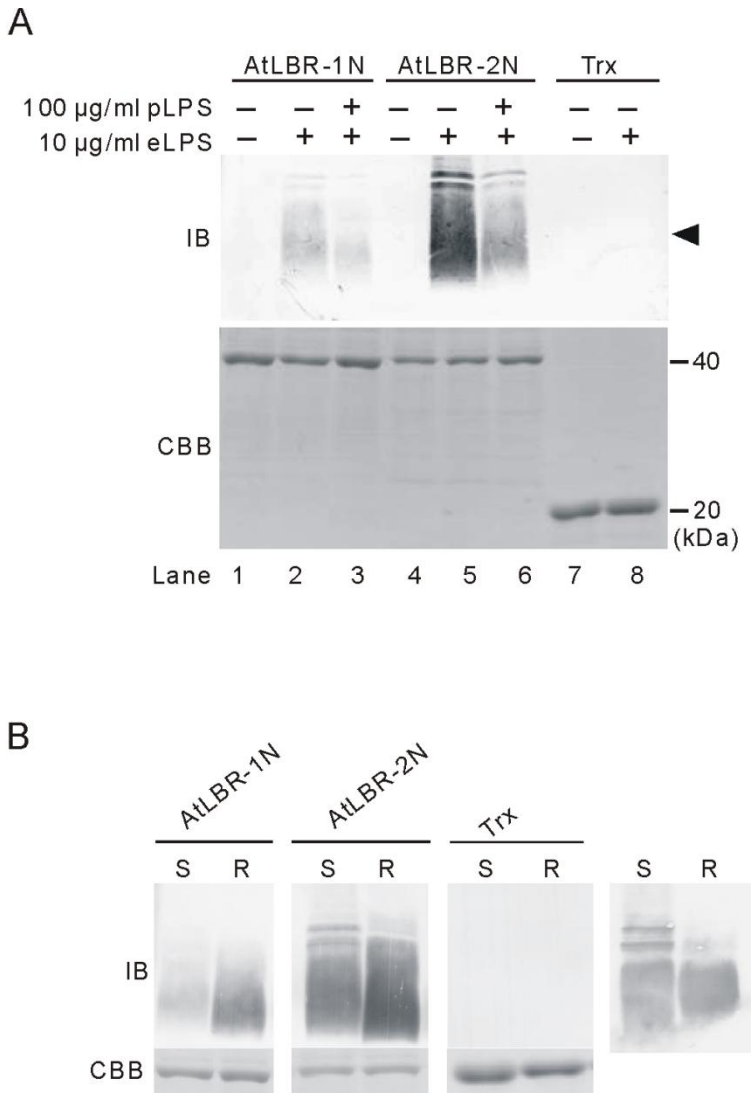

Figure 1-4. Direct binding of AtLBR-1N and AtLBR-2N to LPS.

(**A**) 10 μg/ml LPS-free recombinant proteins were incubated with 10 μg/ml purified eLPS with or without 100 μg/ml purified pLPS. The LPS-protein complexes were purified using His Spin Trap columns and recombinant proteins were analyzed by SDS-PAGE (12% gel) followed by CBB staining (lower panels). eLPS bound to the recombinant protein was detected by anti-eLPS immunoblotting (18% gel, arrowhead) (upper panels). (**B**) 10 μg/ml LPS-free recombinant proteins were incubated with 10 μg/ml smooth (S) and rough (R) LPS from *E. coli*. The binding of the proteins to S and R LPS was examined as above. S and R LPS (100 ng per lane) were used as controls (right panel).

Cellular localisation and expression pattern of AtLBRs.

In many cases, plant pathogens proliferate in the leaf apoplast, thus a number of PAMPs and other extracellular elicitors are also present in the apoplast [24]. Therefore, the apoplast is an important place for plant–pathogen interactions to occur that exclude pathogens. It contains antimicrobial proteins such as proteases, glucanases, chitinases, and chitin-binding proteins. Furthermore, apoplastic ROS generation can function as signalling molecules for plant innate immune responses [24]. Therefore, I analyzed the subcellular localisation of AtLBRs to determine whether or not AtLBRs are expressed in the apoplast. The AtLBR-super folder GFP (sfGFP) construct was introduced into onion epidermal cells by particle bombardment. Transient expression of the fusion protein was observed with a confocal laser-scanning microscope. To observe the apoplastic region, 20% sucrose was used to induce plasmolysis before observation. AtLBR-1-sfGFP and AtLBR-2-sfGFP proteins were co-localised with DsRed protein, which is a cytosolic marker; the fluorescent signals were also detected in vacuolar regions (Fig. 1-5A, B). When the regions of plasmolysis were observed, AtLBR-2-sfGFP, but not AtLBR-1-sfGFP, was detected in the apoplastic region (Fig. 1-5B). This result suggests that AtLBR-1 and AtLBR-2 may function specifically in different expression sites, and AtLBR-2 may play an important role in LPS-induced innate immune responses in the apoplast. As AtLBRs can bind to LPS directly *in vitro*, I investigated the

possible involvement of AtLBRs in the LPS-induced innate immune responses *in vivo*. First, I analyzed gene expression of *AtLBRs* in *Arabidopsis* seedlings (Fig. 1-5C). After whole seedlings were treated with pLPS for 24 and 48 h, *AtLBR* expression was analyzed by quantitative RT-PR (qRT-PCR). The amount of *AtLBR-1* mRNA was not affected by pLPS treatment. In contrast, *AtLBR-2* mRNA level was increased by pLPS treatment (Fig. 1-5C).

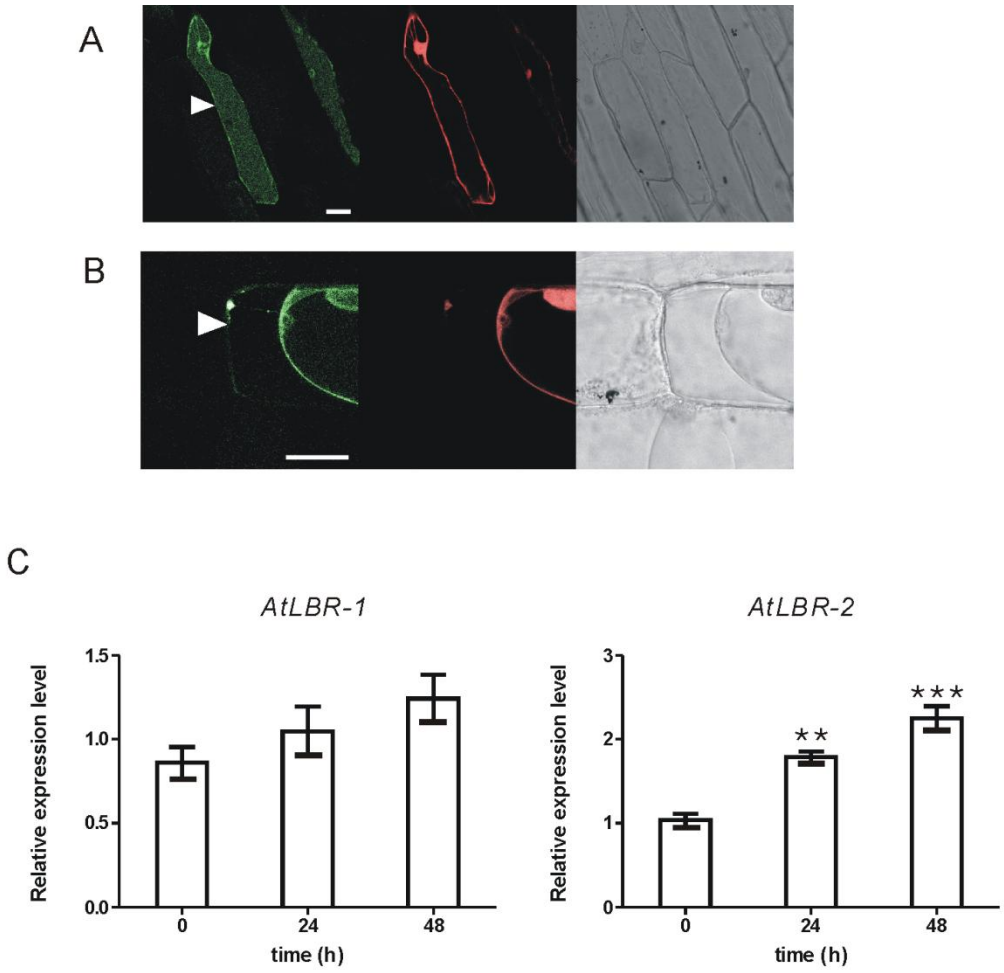

Figure 1-5. Cellular localisation and expression pattern of AtLBRs.

The AtLBR-1-sfGFP (**A**) and AtLBR-2-sfGFP (**B**) fusion proteins were transiently expressed in onion epidermal cells by particle bombardment, and observed with a confocal laser-scanning microscope. Co-bombarded DsRed-monomer was used as a cytosolic marker protein. The arrowhead indicates a plasmolysed cell (**A**) and the apoplastic region (**B**). Scale bar, 50 µm. (**C**) *AtLBRs* mRNA levels in WT *Arabidopsis* seedlings treated with 100 µg/ml pLPS for 24 or 48 h were detected by qRT-PCR. Mean expression values were calculated from the results of three independent experiments. Means ± standard errors are presented. Significant differences among means compared to 0 h treated *Arabidopsis* seedlings were determined by one-way ANOVA followed by *post hoc* Tukey's multiple comparison test. $^{**}P < 0.01$, $^{***}P < 0.001$.

***Arabidopsis atlbr* mutants showed defects in up-regulation of *pathogenesis-related 1* (*PR1*) gene expression and ROS generation induced by LPS.**

To elucidate the relationship between the biological function of AtLBRs and LPS-induced defense responses in plants, I obtained three AtLBR T-DNA insertion lines from the Arabidopsis Biological Resource Center (ABRC) (Fig. 1-6A). *SC815603* (*atlbr-1*) carries a T-DNA insert in *At1g04970*. *SALK_050219* (*atlbr-2-1*) and *SALK_132326* (*atlbr-2-2*) carries a T-DNA insert in *At3g20270*. T-DNA insertion abolished expression of the *AtLBR* mRNA when examined by semiquantitative RT-PCR (Fig. 1-6B). I also generated a *atlbr-1/-2-1* double mutant (*atlbr-DKO*) by crossing *atlbr-1* and *atlbr-2-1*.

Since previous studies reported that LPS treatment induces some *PR* gene expression in *Arabidopsis* [1, 25, 26], I first examined *PR1*, *PR2*, *PR3*, *PR4*, and *PR5* expression in wild-type (WT) *Arabidopsis* by qRT-PCR. pLPS treatment induced expression of *PR1*, *PR4*, and *PR5*, but not of *PR2* and *PR3* in WT (data not shown). Thus, I next investigated *PR1*, *PR4*, and *PR5* expression by qRT-PCR in pLPS-treated *atlbr* mutants. Interestingly, I could detect *PR1* expression in WT but not in *atlbr* mutants at 24 h after pLPS treatments (Fig. 1-7A). However, at later time points of 48 and 72 h, both WT and *atlbr* mutants expressed the *PR1* gene at the same level (Fig. 1-7A, Fig. 1-8). Thus, *atlbr* mutants exhibit a significant delay of *PR1* expression. By using another *PR1* primer set, I also confirmed the delay of *PR1*

gene expression in *atlbr* mutants (Fig. 1-9). In addition, to exclude the possibility of contamination by other bacterial components, I purified commercial pLPS and treated the seedlings with it. The purified pLPS also could induce *PR1* gene expression in WT, while that was defect in *atlbr* mutants (Fig. 1-10). This result excluded the possibility that this phenomenon is caused by contamination. As shown in Fig. 1-7A, I also found significant differences in *PR4* expression between WT and the two mutants, *atlbr-2-1* and *atlbr-DKO*, at 48 h after pLPS treatment. More research focusing specifically on the phenomenon is needed; however, since no difference was observed in *atlbr-2-2*, I tentatively concluded that this phenomenon might not be related to AtLBR-2 function. Thus, the deficiency of pLPS-induced *PR* gene expression in *atlbr* mutants is restricted only to *PR1* gene expression. As shown in Fig. 1-7B, both WT and mutant seedlings similarly induced the expression of *PR1* in response to 1 μM flg22, the bacterial flagellin peptide. This result demonstrates that AtLBR-mediated *PR1* induction is LPS specific. Further, I tested ROS generation as an early response to pLPS (Fig. 1-11A). Although ROS generations were induced equally well by flg22 treatments with both WT and mutants (Fig. 1-11B), those induced by pLPS treatments were significantly reduced in mutants. These results indicate that AtLBRs play important roles in LPS-induced *PR1* expression and ROS production, and suggest that AtLBRs play roles similar to those of hLBP, whose LPS binding facilitates LPS responses.

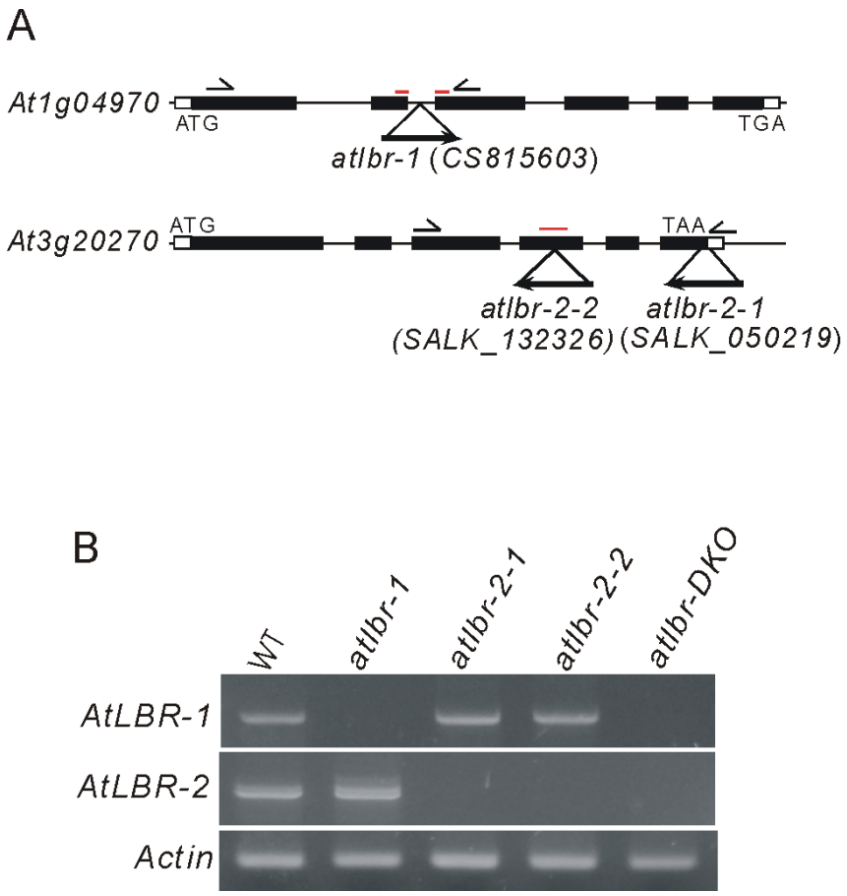

Figure 1-6. T-DNA insertion abolished expression of the *AtLBR* mRNA.

(**A**) T-DNA insertion sites in *atlbr-1, atlbr-2-1,* and *atlbr-2-2* with exons shown as black boxes. RT-PCR primers were designed to amplify the region containing the positions of T-DNA insertion (arrowhead). The orange bar represents the qRT-PCR primer extension site. (**B**) RT-PCR analysis of *AtLBR-1*, *AtLBR-2,* and *Actin* (control) transcripts in WT, *atlbr-1*, *atlbr-2-1*, *atlbr-2-2*, and *atlbr-DKO* plants.

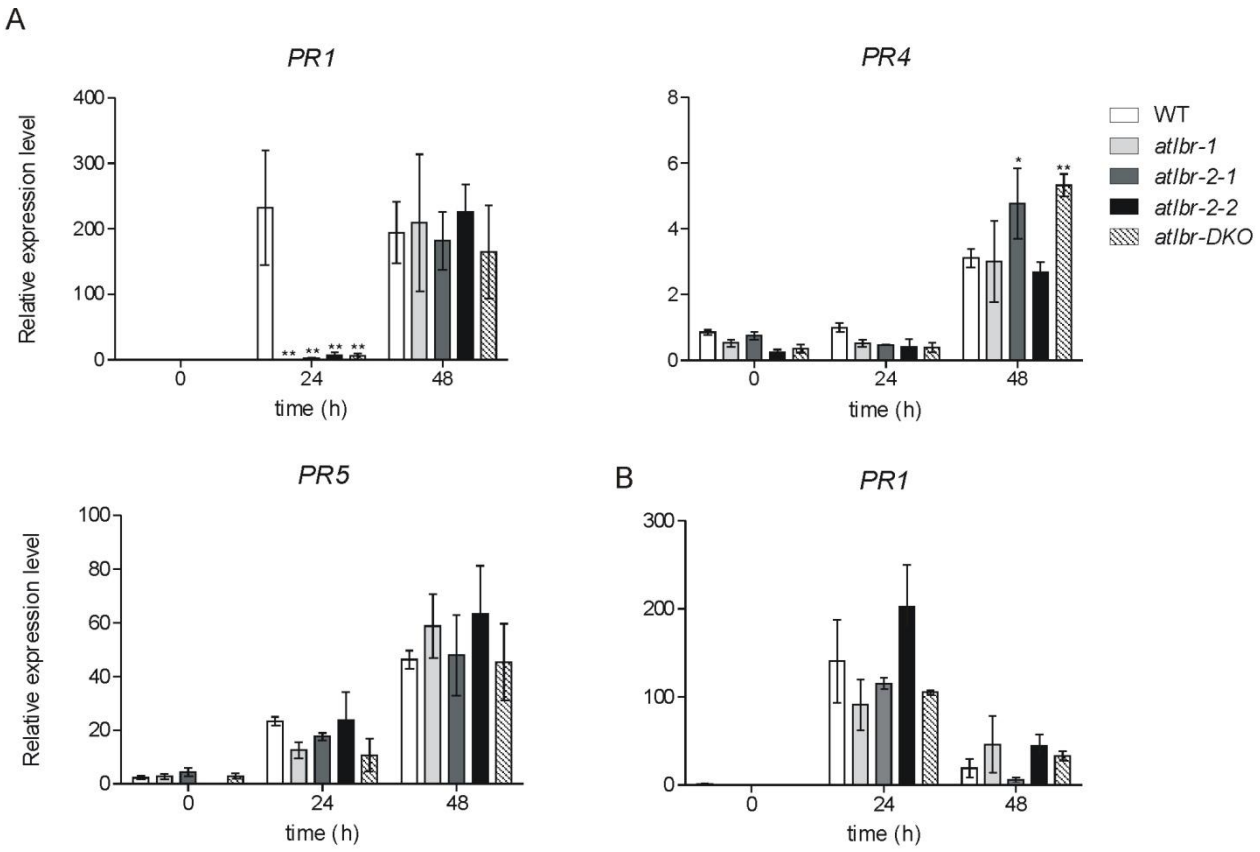

Figure 1-7. Defect in LPS-induced *PR1* gene expression in *atlbr* mutants.

Transcript levels of the *PR* genes were determined by qRT-PCR with cDNA generated from WT and mutants seedlings treated with 100 µg/ml pLPS (**A**) or 1 µM flg22 (**B**) for the indicated time. Mean expression values were calculated from the results of three independent experiments. Means ± standard errors are presented. Significant differences among means were determined by two-way ANOVA followed by *post hoc* Bonferroni tests compared to WT plants; **P* < 0.05, ***P* < 0.01.

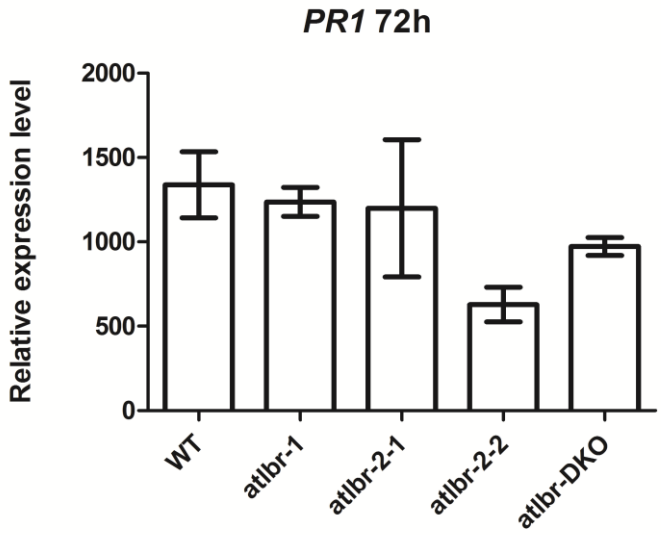

Figure 1-8. *PR1* mRNA levels in WT and *atlbr* mutants *Arabidopsis* seedlings treated with 100 μg/ml pLPS during 72 h were detected by qRT-PCR.

Mean expression values were calculated from the results of three independent experiments. Error bars show means ± s.e.m. Groups were tested by one-way ANOVA followed by Tukey's multiple comparison test comparing with WT plants.

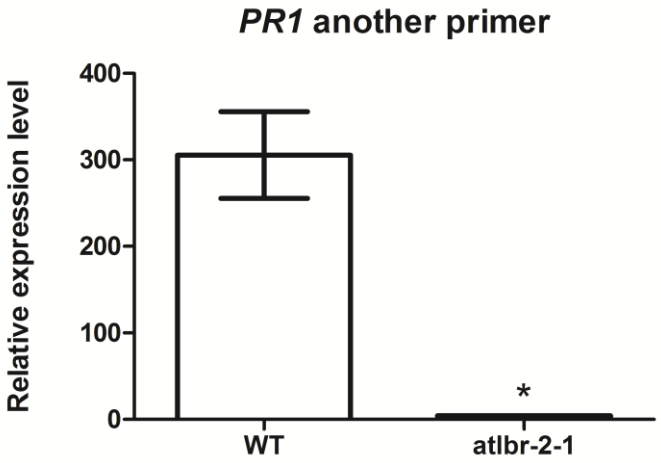

Figure 1-9. *PR1* mRNA levels in WT and *atlbr-2 Arabidopsis* seedlings treated with 100 μg/ml pLPS during 24 h were detected by qRT-PCR using another set of primers (Table 1-1).

Mean expression values were calculated from the results of three independent experiments. Error bars show means ± s.e.m. *$P < 0.05$ by t test.

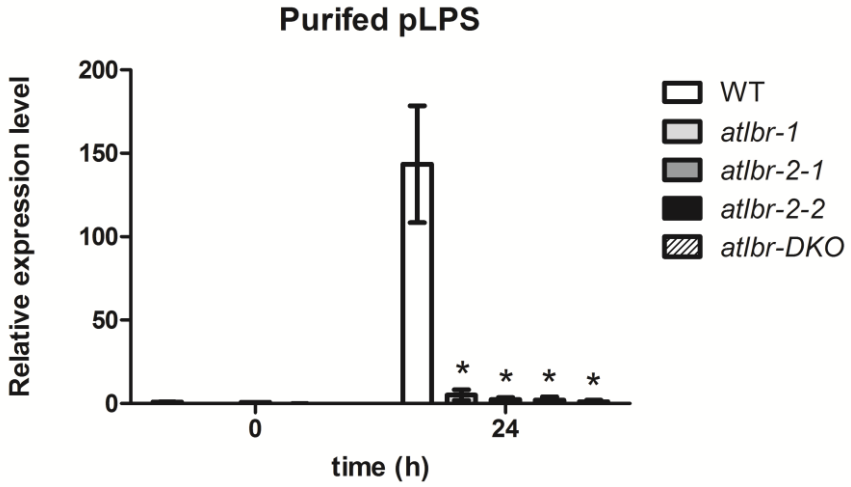

Figure 1-10. Purchased *P. aeruginosa* LPS was purified by degradation of nucleic acids and proteins with DNase I, RNase, and proteinase K.

PR1 mRNA levels in WT and *atlbr* mutants *Arabidopsis* seedlings treated with 100 μg/ml purified pLPS during 24 h were detected by qRT-PCR. Mean expression values were calculated from the results of three independent experiments. Error bars show means ± s.e.m. **P* < 0.001 by two-way ANOVA followed by *post hoc* Bonferroni test comparing with WT plants.

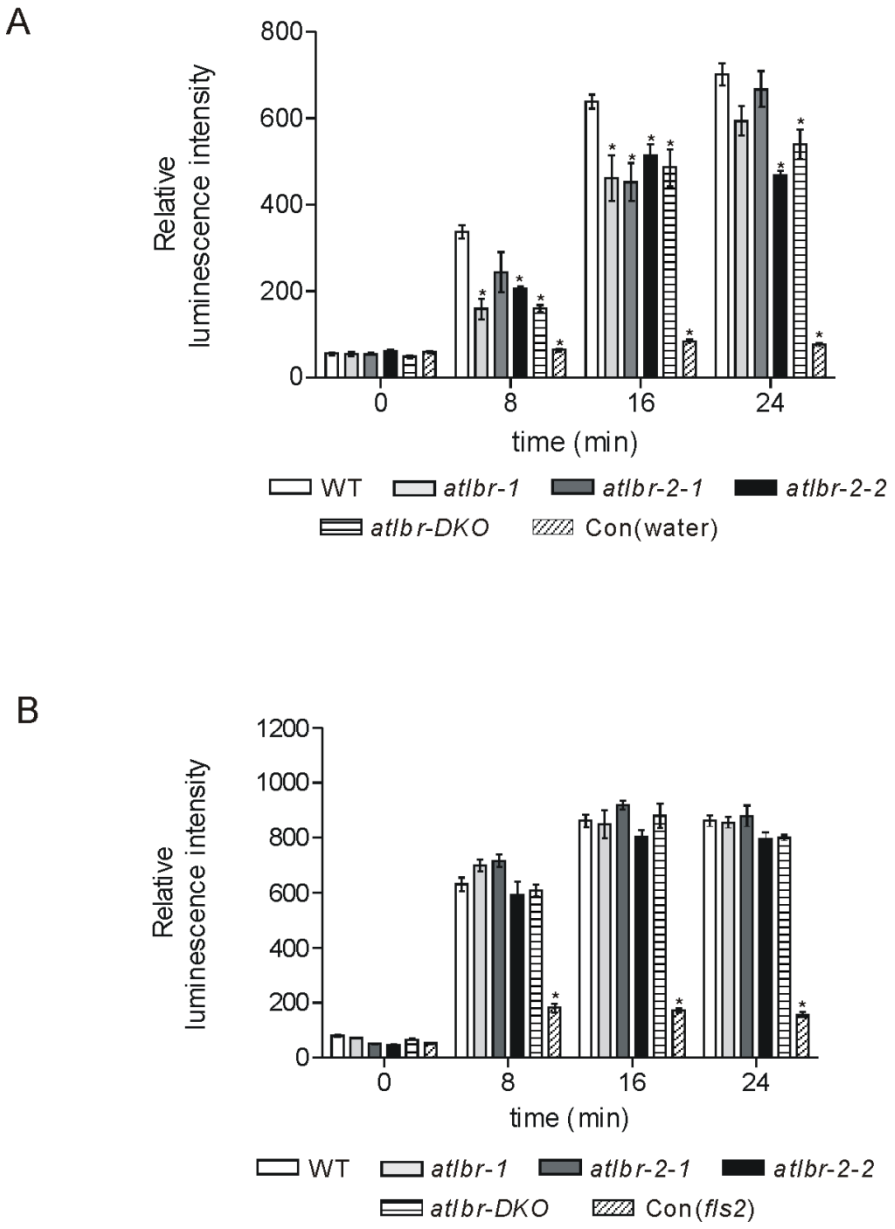

Figure 1-11. Defect in LPS-induced ROS generation in *atlbr* mutants.

ROS generation by leaves of WT and *atlbr* mutants after treatments with 10 µg/ml pLPS (**A**) or 0.1 µM flg22 (**B**) for the indicated time. As a control, WT and *fls2* (FLAGELLIN-SENSITIVE 2) mutant leaves were treated with water and flg22, respectively. Means ± standard deviations are presented (n = 5). Significant differences among means compared to WT plants were determined by two-way ANOVA followed by *post hoc* Bonferroni tests; *$P < 0.01$.

Discussion

Although LBP/BPI/PLUNC superfamily proteins have been identified in various animals including non-mammalian vertebrates and invertebrates [10–15], those of plants have not been defined. In this study, I characterized *Arabidopsis* LBP/BPI subfamily proteins termed AtLBR-1 and AtLBR-2 by analyzing LPS-binding activity and studying the immune response to LPS in plants for the first time.

AtLBRs and other LBP/BPI/PLUNC superfamily

Phylogenetic analyses suggest that *Arabidopsis* AtLBRs are distantly related to mammalian LBP/BPI. However, I demonstrated that AtLBRs appear to have an immunological role similar to LBP/BPI subfamily proteins, including mammalian LBP, BPI, and Cg-BPIs, and PLUNC-related protein OCX-36. This result suggest that the LBP/BPI subfamily proteins with an the immunological role are distributed not only in animals but also in plants. However, the LBP/BPI subfamily also includes two lipid-binding proteins which have roles other than an immunological one; phospholipid transfer protein (PLTP) and cholesteryl ester transfer protein (CETP) play pivotal roles in LDL and HDL metabolism [7, 27, 28], although they have been found only in vertebrates. This finding suggests that LBP/BPI proteins with the lipid-transfer role would have emerged after vertebrates diverged from a common

ancestor. It is important to note that PLTP also shows an immunological role for LPS; it can bind and neutralize LPS [29]. Based on these observations and phylogenetic analyses (Fig. 1-2) the following hypothesis can be proposed: a common ancestor of the LBP/BPI/PLUNC superfamily first played an immunological role, then some descendants acquired functions other than immunological ones (i.e., CETP and PLTP). On the other hand, I cannot exclude a second hypothesis: a common ancestor of the LBP/BPI/PLUNC superfamily first played a lipid-binding role, then its descendants were divided into two major subfamilies: proteins that acquired an immunological role (i.e., LBP, BPI, Cg-BPIs, OCX-36, and AtLBRs) and proteins with a role similar to the original one (i.e., PLTP and CETP).

Structural characterization of AtLBRs

Crystal structure analyses of LBP, BPI, and CETP reveal that each of the N- and C-terminal domains contains a single hydrophobic pocket with a bound phospholipid molecule [18, 30, 31]. Furthermore, CETP has two distinct hydrophobic tunnel openings in each domain, which is capped by one phospholipid [31]. Therefore, AtLBRs are also considered to have the hydrophobic pockets in their N- and C-terminal domains. Based on this finding and the result that N-terminal domains of AtLBRs bind to LPS, the N-terminal hydrophobic pocket may contribute to LPS binding. In addition, given that some LBP/BPI/PLUNC superfamily

proteins bind to phospholipids via the hydrophobic pockets, AtLBRs may bind not only to LPS but also to other phospholipid molecules via these hydrophobic pockets.

AtLBR-binding moiety of LPS

In Chapter 1, I demonstrated the direct binding between AtLBRs and LPS. LPS consists of three distinct structural regions: O-antigen, oligosaccharide core, and lipid A. Although only the lipid A moiety is required for the activation of an immune response in animals, both the lipid A moiety and the O-antigen are important for a response in plants. A previous study revealed that treatment with lipid A induces *PR1* gene expression and NO and ROS production in *Arabidopsis* [1, 4, 25]. However, synthetic oligorhamnans, a common component of the otherwise highly variable O-antigen in LPS, also can trigger defense responses in *Arabidopsis* [26]. In this study, I found that the recombinant AtLBRs could bind to rough type LPS, which lacks O-antigen. This result suggests that O-antigen is not necessary for LPS recognition by AtLBRs. Thus, AtLBRs may affect the recognition of the lipid A moiety to regulate immune responses in plants. However, although the interaction of hBPI with smooth or rough type LPS is not significantly different [22], AtLBRs showed higher binding affinity to rough type than to smooth type, suggesting that the O-antigen might prevent the binding of AtLBRs to the lipid A moiety of LPS.

Localization and functional properties of AtLBRs

Analysis of subcellular localization showed that, in particular, AtLBR-2 was located in the apoplastic region. In addition, LPS-treated *atlbr* mutants showed significant decreases in *PR1* gene expression compared to that in the WT. These findings support the hypothesis that AtLBR-2 binds to LPS and catalyses LPS-induced immune responses in apoplastic space. Thus, AtLBR-2 may have activity similar to LBP rather than to BPI. Thus, similar to mammalian LBP which facilitates transfer of LPS to the TLR4/MD-2 receptor complex to amplify the immune responses against LPS, AtLBR-2 might also facilitate the transfer of LPS to a plant LPS receptor, with LORE being one recently identified candidate [4]. In contrast, although recombinant AtLBR-1N showed LPS-binding activity and *atlbr-1* is defective in LPS-induced *PR1* up-regulation, LPS treatment had not effect on *AtLBR-1* expression and I did not obtain clear localisation of the AtLBR-1-sfGFP fusion protein in the apoplastic region. I predict that AtLBR-1 may bind to LPS molecules and is involved in LPS signalling in intracellular regions such as the cytosol or vacuoles. More research is needed to better understand the relationship between AtLBR-1 and the LPS recognition mechanism in plants.

AtLBRs and SA signaling

I demonstrated the deficiencies of LPS-induced *PR1* gene expression in *atlbr* mutants. However, the deficiencies restricted only expression of *PR1* but not *PR4* or *PR5*. It is well known that *PR* gene expression occurs after PAMP-induced salicylic acid (SA) accumulation [32]. SA is an important signal molecule in plant defense. Downstream of SA, *PR* gene induction occurs via two mechanisms: NON-EXPRESSOR OF PR1 (NPR1)-dependent and -independent pathways [32]. NPR1, a master regulator of SA-mediated defense genes, interacts with basal and systemic acquired resistance in plants. In the NPR1-dependent SA-induced pathway, *PR1* gene expression was observed. In contrast, in the NPR1-independent SA-induced pathway, expression of *PR2* and *PR5* genes was observed [33]. These findings led to the hypothesis that AtLBRs are involved in the NPR1-dependent SA-induced pathway. In *atlbr* mutants, I detected the expression of *PR4*, the marker for ethylene (ET) signalling, suggesting that *atlbr* mutations had no effect on LPS-induced ET signalling.

It has been reported that SA signalling is preceded by ROS bursts mediated by NADPH oxidases and extracellular peroxidases [34]. ROS signals are involved in both upstream and downstream SA signalling in response to biotic and abiotic stress, including PAMPs, ozone, and UV-B treatment [34]. In this study, I showed that ROS generation significantly differed between pLPS-treated WT and *atlbr* mutants. The relatively low level

of ROS generation in *atlbr* mutants may be one of the causes for deficiencies in *PR1* expression.

This Chapter 1 study is the first to demonstrate that AtLBRs share functional similarities with the other LBP/BPI subfamily proteins. My results suggest that plants have mechanistic parallels with animals for LPS perception.

Materials and Methods

Elicitors. Rough and smooth LPS from *E. coli* were prepared from the Origami B strain (DE3) (Novagen) and the ATCC 25922 strain, respectively, as reported previously [19]. LPS from *Pseudomonas aeruginosa* serotype 10 was purchased from Sigma-Aldrich. The elicitor peptide flg22 was synthesised by Biologica Co.

Sequence analysis. Protein sequences were obtained from NCBI: AtLBR-1 (NM_100375), AtLBR-2 (NP_188662), hLBP (CAA67226), and hBPI (ABD66755). Alignment was performed with Clustal-W implemented in BioEdit version 7. 0. 8. 0. (www.mbio.ncsu.edu/bioedit/bioedit.html). Conserved domain analyses were carried out using Conserved Domain Databases (http://www.ncbi.nlm.nih.gov/cdd/).

cDNA cloning and plasmid construction. In the construction of the vector for protein expression in *E. coli*, RNA was extracted from *Arabidopsis* using the plant total RNA extraction Miniprep system (Viogene). DNase-treated RNA (3.75 μg) was reverse-transcribed using random primers (TAKARA BIO) and Superscript II reverse transcriptase (Invitrogen) according to the manufacturer's protocol. cDNA fragments for N-terminal AtLBR-1 (AtLBR-1N) coding 215 amino acid residues (1–215) were amplified by PCR using PrimeSTAR GXL DNA Polymerase (TAKARA BIO). Amplification was first carried out with nested primer set Nes1n, followed by primer set ATLBR-1n (Table 1-1). cDNA fragments for N-terminal AtLBR-2 (AtLBR-2N) coding 214 amino acid residues (1–214) were also created as described above using nested primer set Nes2n and primer set ATLBR-2n (Table 1-1). For expression as a N-terminal thioredoxin (Trx) and His-tag fusion protein, these fragments were also amplified using primer set pSU2amp (Table 1-1), then they were cloned into pET32a(+) by yeast recombinational cloning using pYES2/CT as a helper plasmid [35]. The nucleotide sequences of these recombinant proteins were confirmed by sequencing using an ABI 310 genetic analyzer (Applied Biosystems). A fusion protein of Trx with His-tags was used as a control in this study. For the subcellular localization analysis,

I cloned cDNA of full-length AtLBR-1 and the genomic sequence of AtLBR-2 into P35S-sfGFP-TNos vector [36] by yeast homologous recombination [37].

Protein expression and purification. Protein expression and purification were performed based on a method reported previously [19]. In brief, Origami B (DE3) was transformed with the plasmids and cultured. Extraction was performed using a French Pressure Cell Press (Otake Seisakusho). The supernatants were applied to a nickel-absorbed chelating sepharose column. After washing with the buffer, including 50 mM imidazole with or without 0.5% TX-100, adsorbed proteins were eluted with the same buffer, changing the concentration of imidazole to 500 mM. The protein preparations were analyzed by SDS-PAGE (12% acrylamide gel) and Coomassie brilliant blue (CBB) staining. Detection of LPS was performed by immunoblotting (18% acrylamide gel) using an anti-LPS monoclonal antibody NW1 222-5 (Hycult Biotechnology), alkaline phosphatase-conjugated anti-mouse Ig (American Qualex), and BCIP/NBT Colour Development Substrate (Promega) [19].

LPS-binding assay and competition test. This procedure is based on a method published previously [19]. LPS-free recombinant proteins were prepared by affinity chromatography on Ni-columns using a washing buffer containing 0.5% TX-100. Recombinant proteins were

diluted to 10 μg/ml in a buffer (50 mM phosphate buffer, pH 7.0, 150 mM NaCl, 50 mM imidazole, 1 mM PMSF, 5 mM 2-ME, and 1 mg/ml of BSA) and incubated at room temperature for 30 min with 10 μg/ml LPS from *E. coli* (smooth type). In the competition test, recombinant proteins were incubated with 10 μg/ml smooth type LPS from *E. coli* with or without 100 μg/ml LPS from *P. aeruginosa*. The mixtures were applied to His Spin Trap columns (GE Healthcare), washed, and eluted according to the manufacturer's protocol by using the same buffers used in the column chromatography. Without dilution, eluted samples were analyzed to determine LPS content by immunoblotting.

Subcellular localization analysis. An appropriate plasmid mix for expression of sfGFP fusion and DsRed-monomer proteins was co-bombarded with gold particles by the biolistic particle delivery system (PDS-1000/He, Bio-Rad) into onion (*Allium cepa*) epidermal cell layers. The DsRed-monomer was used as a cytosolic marker protein. After incubation at 23 °C for 16 h in darkness, fluorescence images were obtained with a confocal microscope (TCS SP8, Leica). A white light laser was used for the excitation lights (488 and 556 nm for sfGFP and DsRed-monomer, respectively). The emission signals were captured at 498–549 nm for sfGFP and at 566–650 nm for DsRed-monomer. To induce plasmolysis, the onion

epidermal cell layers were treated with 20% sucrose solution for 10 min before the microscopic observation.

Plant material and growth conditions. *Arabidopsis* ecotype Col-0 was used as a control in this study. T-DNA insertion line CS815603 (*atlbr-1*) was provided by SAIL (Syngenta *Arabidopsis* Insertion Library). T-DNA insertion lines SALK_050219 (*atlbr-2-1*) and SALK_132326 (*atlbr-2-2*) were provided by SIGnAL (Salk Institute Genomic Analysis Laboratory). All plants were in the Col background. *atlbr-DKO* double knockout mutants were obtained by crossing *atlbr-1* and *atlbr-2-1* mutants. AtLBR-1-, AtLBR-2- and T-DNA-specific primers were used to select plants homozygous for the insert. All plant were grown at 22–24 °C with a 16 h light/−8 h dark cycle.

Elicitor treatment and qRT-PCR analysis. After seedlings were grown for 5 days on MS agar plates under the conditions defined above, they were transferred to liquid MS medium supplied with the indicated elicitor preparations under continuous light conditions. After elicitor treatment, whole seedlings were ground to a powder in liquid nitrogen. RNA was extracted and reverse transcribed using 1 μg of total RNA. qRT-PCR was run on a PikoReal real-time PCR system (Thermo Fisher Scientific) according to the manufacturer's

recommendations with the following conditions: 1 cycle of 1 min at 95 °C, and 40 cycles of 5 s at 95 °C and 30 s at 60 °C. *β-Tubulin4* was used as an internal standard. The gene-specific primers were used as described [38] (Table 1-1). Each experiment was repeated at least three times.

ROS measurements. ROS generation was determined using the H_2O_2-dependent chemiluminescence reaction based on a method reported previously [39]. *Arabidopsis* leaves of 3- to 4-week-old plants grown on MS agar plates were cut into 2 mm slices and floated on H_2O overnight. Slices (20 mg fresh weight) were exposed to elicitor solutions, and 2 μl of the solution was transferred to assay tubes containing 0.1 ml of H_2O supplemented with 20 μM luminol and 1 μg horseradish peroxidase (Sigma). Luminescence was measured in a GloMax 20/20 Luminometer (Promega) for 28 min after treatment.

Table 1-1. Primers set used in Chapter 1.

For AtLBRs cloning and plasmid construction.

Set	F/R	Sequence
ATLBR-1n	F	5’-TTCGAGCTCCGTCGAACCGATTCATTCACATCGGT-3’
	R	5’-AGCAGCCGGATCTCATTATATAGGATCACTGGTGA-3’
ATLBR-2n	F	5’-TTCGAGCTCCGTCGAAACAATGGCGGTCACATTTC-3’
	R	5’-AGCAGCCGGATCTCATTAGACAGGGTTGCCTGTAA-3’
Nes1n	F	5’-CCAAGTTTCTTCTTCTTGCC-3’
	R	5’-GTGAAAACTCTAACTACCGA-3’
Nes2n	F	5’-TCTTCGTCTCGGTGTCATCG-3’
	R	5’-GCCAACTTCAACTGTAGTTA-3’

pSU2amp	F	5’-GGCCATGGCTGATATCGGATCCGAATTCGAGCTCCGTCGA-3’
	R	5’-ACTCAGCTTCCTTTCGGGCTTTGTTAGCAGCCGGATCTCA-3’

For semiquantitative RT-PCR.

Set	**F/R**	**Sequence**
RT-AtLBR1	F	5’-GCACCGATTCATTCACATCG-3’
	R	5’-CCTTTGGAAGGCTTTGTAGG-3’
RT-AtLBR2	F	5’-GGTGGTTGATGCATTTCAAA-3’
	R	5’-CTTCAGGCTTACGTACATGC -3’
RT-Actin	F	5’-TCTTGATCTTGCTGGTCGTG-3’
	R	5’-GAGCTGGTTTTGGCTGTCTC-3’

For qRT-PCR.

Set	**F/R**	**Sequence**
qAtLBR-1	F	5’- CCATTGAGTTGGAAGGAGGA-3’
	R	5’- TGGCAATGGTACTTTCCACA-3’
qAtLBR-2	F	5’- CGGGTCCATTCTAAGCACAT-3’
	R	5’- ATCGTCGCATCAATTCCATT-3’
qPR1	F	5’- GGAGCTACGCAGAACAACTAAGA-3’
	R	5’- CCCACGAGGATCATAGTTGCAACTGA-3’
qPR4	F	5’- TTGCTCCACGTGGGATGCTGAT-3’
	R	5’- AGCTCATTGCCACAGTCGACAA-3’
qPR5	F	5’- CGGTACAAGTGAAGGTGCTCGTT-3’
	R	5’- GCCTCGTAGATGGTTACAATGTCA-3’
qβ-Tubulin4	F	5’- GAGGGAGCCATTGACAACATCTT-3’
	R	5’- GCGAACAGTTCACAGCTATGTTCA-3’

For Figure 1-8 (another set of *PR1* primers).

Set	**F/R**	**Sequence**
qPR1-2	F	5’- GTCTTTGTAGCTCTTGTAGGTG-3’
	R	5’- CAACCCTCTCGTCCCACTGCAT-3’

Chapter 2:

Transcriptome analysis reveals key roles of AtLBR-2 in LPS-induced defense responses in plants

Introduction

In Chapter 1, I identified two *Arabidopsis* LBP/BPI-related proteins, AtLBR-1 and AtLBR-2 [40]. When I incubated recombinant forms of both AtLBR-1 and AtLBR-2 with pLPS separately, they exhibited the capability to bind to it directly; *atlbr* mutants showed deficiencies in pLPS-induced *PR1* gene expression and ROS generation. I predicted that AtLBR-2 would be more important than AtLBR-1 in the induction of defense responses to LPS because the binding affinity of AtLBR-2 for LPS appeared higher than that of AtLBR-1, and AtLBR-2 is located in the apoplastic region.

In this Chapter 2, I investigated the importance of AtLBR-2 in the dynamic changes in *Arabidopsis* transcriptome in response to LPS treatment. To achieve this goal, I performed a transcriptome analysis using high-throughput mRNA sequencing (RNA-Seq). RNA-Seq analysis using WT and the *atlbr-2-1* identified 65 AtLBR-2-dependent genes that were up-regulated after LPS treatment. These 65 genes appear to be important for the enrichment of some defense-related gene ontology (GO) terms. My findings highlight the indispensable

role of AtLBR-2 in defense signaling mechanism against LPS.

Results

Transcriptomic analysis of *P. aeruginosa* LPS-responsive genes in WT *Arabidopsis*.

To examine and compare the LPS-induced transcriptional changes between WT and the *atlbr-2-1*, I treated them with pLPS; total RNA was extracted and RNA-Seq analysis was performed.

Firstly, I analyzed the pLPS-responsive genes in the WT. The RNA-Seq data obtained from untreated WT were compared with that of pLPS-treated WT. I observed that the transcript levels of 2,139 genes changed significantly in pLPS-treated WT. Of these, 605 genes were identified as up-regulated genes in pLPS-treated WT (Fig. 2-1A). Moreover, 1,534 genes were identified as down-regulated genes in pLPS-treated WT (Fig 2-1B). I performed gene ontology (GO) analysis of these genes using the functional annotation chart of DAVID. The biological process (BP) GO classification of the 605 up-regulated genes identified 33 GO terms ($P < 0.01$, Fig. 2-2, blue line) (Table 2-1), including not only defense-related GO terms, but also several metabolic processes-related terms. This finding corresponded with the results reported from transcriptional analysis on *Arabidopsis* seedlings treated with LPS from *Burkholderia cepacia* [41]. Defense-related GO terms included,

“response to bacterium”, “response to SA stimulus”, “response to abscisic acid (ABA) stimulus”, “response to jasmonic acid stimulus”, “response to ROS”, and “response to wounding”. In contrast, 1,534 down-regulated genes were classified via 43 GO terms ($P < 0.01$) (Table 2-2). Interestingly, defense-related GO terms, other than “response to bacterium”, “response to SA stimulus”, “response to ABA stimulus”, were also common in these 43 GO terms. These findings suggested that up-regulation, but not down-regulation, of genes related to bacterial responses may be a characteristic of normal pLPS-induced gene expression. It can also be inferred that SA- and ABA-related pathways may be important for the up-regulation, but not down-regulation, of genes after pLPS treatment.

Furthermore, cellular component (CC) GO analysis showed that 23.0% of the 605 up-regulated genes were categorized as “endomembrane system”; also, 22.9% and 11.9% of the 1,534 down-regulated genes were categorized as “endomembrane system” and “intrinsic to membrane”, respectively (Table 2-3). These results indicated that genes activated in the membrane-related region were most affected by the pLPS treatment.

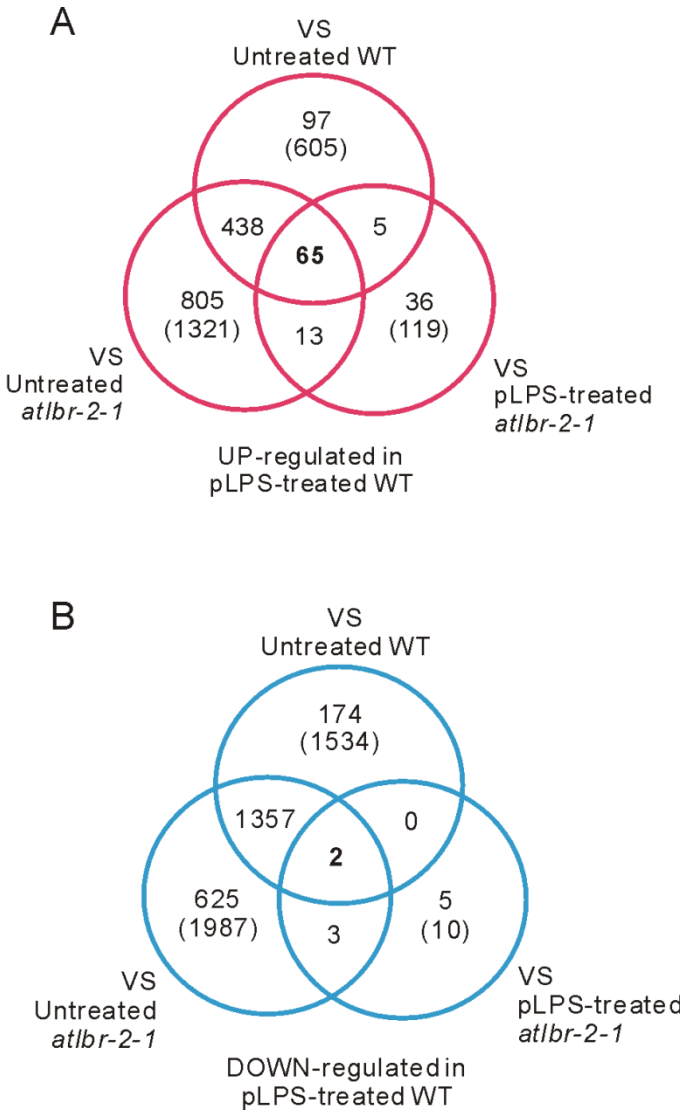

Figure 2-1. The number of differentially expressed genes in pLPS-treated WT plants.
Each RNA-Seq data set obtained from untreated WT, pLPS-treated *atlbr-2-1*, and untreated *atlbr-2-1* plants, were compared with that obtained from pLPS-treated WT plants. The numbers in the parentheses indicate the number of genes identified as up-regulated (**A**) or down-regulated (**B**) in the pLPS-treated WT plants. The numbers of genes, which were up- or down-regulated only in pLPS-treated WT but not in the other three conditions, are indicated in bold type.

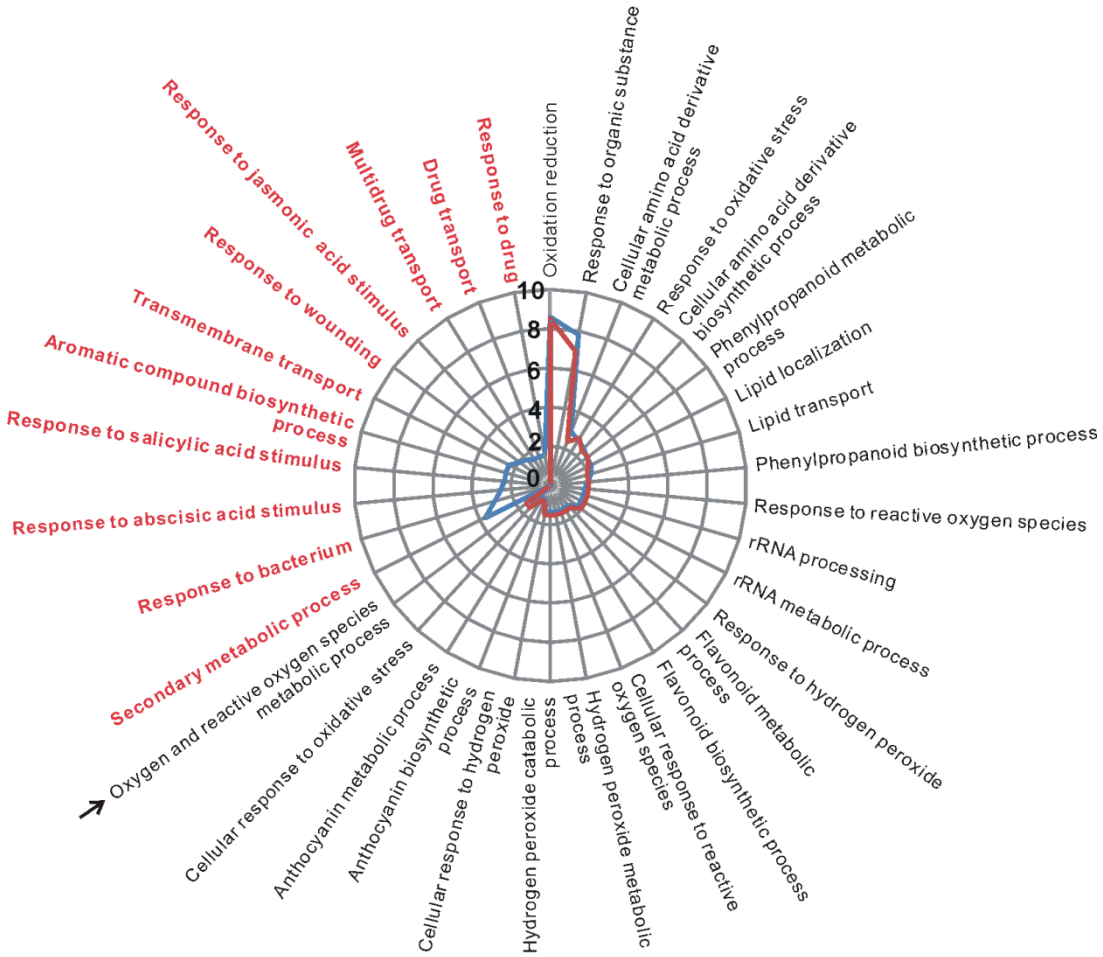

Figure 2-2. GO classification of pLPS-responsive up-regulated genes.

BP GO terms obtained from the GO analysis of 605 pLPS-induced up-regulated genes in WT are shown with the blue line. The same analysis conducted with 540 genes, which excluded 65 AtLBR-2-dependent up-regulated genes from the 605 genes, are shown with the red line. The red font highlights no enriched GO terms in the 540 genes. An arrow indicates the GO term identified only in 540 genes. Scale of y axis shows the percentage of genes that are annotated for each biological process. $P < 0.01$.

Table 2-1. Gene ontology (GO) analysis of the 605 and 540 pLPS-induced up-regulated genes from WT plants using the functional annotation chart of DAVID (*P* < 0.01).

BP GO Term	605 genes		540 genes	
	%	***P*-Value**	%	***P*-Value**
Oxidation reduction	8.593750	2.76E-05	8.496732	6.53E-05
Response to organic substance	7.812500	4.32E-04	6.971678	0.007049
Cellular amino acid derivative metabolic process	2.929688	9.50E-04	2.396514	0.002579
Response to oxidative stress	2.734375	0.003404	2.832244	0.003169
Cellular amino acid derivative biosynthetic process	2.539063	3.39E-04	2.396514	0.001554
Phenylpropanoid metabolic process	2.343750	3.33E-04	2.396514	4.65E-04
Lipid localization	2.343750	3.16E-04	2.178649	0.001781
Lipid transport	2.148438	5.02E-04	1.960784	0.003210
Phenylpropanoid biosynthetic process	1.953125	7.52E-04	1.960784	0.001347
Response to reactive oxygen species	1.757813	0.005292	1.960784	0.002375
rRNA processing	1.757813	0.002402	1.960784	0.001042
rRNA metabolic process	1.757813	0.002402	1.960784	0.001042
Response to hydrogen peroxide	1.757813	0.001753	1.960784	7.51E-04
Flavonoid metabolic process	1.367188	7.17E-04	1.525054	3.56E-04
Flavonoid biosynthetic process	1.367188	4.83E-04	1.525054	2.38E-04
Cellular response to reactive oxygen species	1.367188	0.009456	1.525054	0.005058
Hydrogen peroxide metabolic process	1.367188	0.006577	1.525054	0.003471
Hydrogen peroxide catabolic process	1.367188	0.005563	1.525054	0.002919
Cellular response to hydrogen peroxide	1.367188	0.005563	1.525054	0.002919
Anthocyanin biosynthetic process	0.781250	7.38E-04	0.87146	5.01E-04
Anthocyanin metabolic process	0.781250	0.002115	0.87146	0.001447
Cellular response to oxidative stress	1.367188	0.009930	1.525054	0.005322
Oxygen and reactive oxygen species metabolic process	0.000000	—	1.525054	0.009738
Secondary metabolic process	3.710938	0.001235	0.000000	—
Response to bacterium	2.929688	2.42E-04	0.000000	—
Response to abscisic acid stimulus	2.539063	0.008461	0.000000	—
Response to salicylic acid stimulus	2.343750	1.37E-04	0.000000	—
Aromatic compound biosynthetic process	2.343750	0.002747	0.000000	—

Transmembrane transport	2.343750	0.002650	0.000000	—
Response to wounding	1.953125	0.001988	0.000000	—
Response to jasmonic acid stimulus	1.757813	0.009934	0.000000	—
Multidrug transport	1.562500	5.45E-04	0.000000	—
Drug transport	1.562500	8.06E-04	0.000000	—
Response to drug	1.562500	8.68E-04	0.000000	—

Table 2-2. GO analysis of the 1,534 pLPS-induced down-regulated genes from WT plants using the functional annotation chart of DAVID (*P* < 0.01).

BP GO Term	%	*P*-Value
Response to organic substance	9.309091	1.40E-15
Oxidation reduction	7.781818	3.03E-08
Defense response	7.272727	2.31E-09
Response to endogenous stimulus	7.127273	5.51E-10
Transcription	6.690909	0.003425
Response to hormone stimulus	6.254545	1.23E-07
Intracellular signaling cascade	6.181818	3.73E-10
Response to abiotic stimulus	6.109091	0.005501
Response to oxidative stress	3.490909	2.90E-12
Cellular response to hormone stimulus	3.200000	4.36E-05
Hormone-mediated signaling	3.200000	4.36E-05
Response to carbohydrate stimulus	2.981818	1.47E-13
Immune response	2.909091	8.44E-08
Death	2.690909	5.42E-08
Cell death	2.690909	5.42E-08
Response to auxin stimulus	2.690909	4.25E-05
Innate immune response	2.618182	1.14E-06
Response to chitin	2.472727	9.13E-15
Response to ethylene stimulus	2.181818	8.20E-05
Response to reactive oxygen species	2.181818	1.60E-10
Programmed cell death	2.181818	6.13E-06
Two-component signal transduction system (phosphorelay)	2.109091	1.12E-05
Response to hydrogen peroxide	2.036364	5.08E-11
Ethylene mediated signaling pathway	1.890909	2.97E-06
Apoptosis	1.890909	3.68E-06
Response to water deprivation	1.672727	1.43E-04
Response to water	1.672727	2.94E-04
Cellular response to oxidative stress	1.600000	1.97E-08
Oxygen and reactive oxygen species metabolic process	1.600000	2.01E-07
Cellular response to reactive oxygen species	1.527273	8.45E-08
Cellular response to hydrogen peroxide	1.454545	6.44E-08
Hydrogen peroxide catabolic process	1.454545	6.44E-08

Hydrogen peroxide metabolic process	1.454545	1.16E-07
Response to wounding	1.381818	7.17E-04
Response to heat	1.309091	3.54E-04
Response to jasmonic acid stimulus	1.309091	0.003517
Response to light intensity	1.163636	4.79E-06
Plant-type cell wall organization	1.163636	1.13E-05
Response to high light intensity	0.945455	1.84E-06
Response to glucose stimulus	0.509091	0.001562
Response to hexose stimulus	0.509091	0.001941
Response to monosaccharide stimulus	0.509091	0.001941
Response to fructose stimulus	0.363636	7.76E-04

Table 2-3. Cellular component (CC) GO analysis of pLPS-induced up- or down-regulated genes from WT plants using the functional annotation chart of DAVID (*P* < 0.01).

605 pLPS-induced up-regulated genes CC GO Term	**%**	***P*-Value**
Endomembrane system	23.046875	6.58E-05
External encapsulating structure	4.882813	0.003017
Apoplast	3.320313	0.006991

1534 pLPS-induced down-regulated genes CC GO Term	**%**	***P*-Value**
Endomembrane system	22.909091	2.60E-22
Anchored to membrane	2.618182	5.74E-06
Extracellular region	6.472727	1.02E-04
Intrinsic to membrane	11.927273	4.92E-04
Cell wall	3.272727	0.005532
Extracellular space	0.363636	0.006245
Plant-type cell wall	1.745455	0.006290
External encapsulating structure	3.272727	0.007014

Identification of AtLBR-2-dependent up- or down-regulated genes.

To elucidate the importance of AtLBR-2 in pLPS-induced transcriptional responses, I identified the genes that were up-regulated in an AtLBR-2-dependent manner after 24 h of pLPS treatment. I compared each of the three RNA-Seq data with that of pLPS-treated WT (Fig. 2-1). Furthermore, I studied the genes that were up- or down-regulated only in the pLPS-treated WT plants and not in the other 3 data sets; these were then identified as AtLBR-2-dependent up- or down-regulated genes. A total of 65 candidate genes were identified to be AtLBR-2-dependent up-regulated genes (Fig. 2-1A, Table 2-4). I focused on these 65 genes and analyzed them further; only two genes, "*unfertilized embryo sac 11* (*UNE11*: AT4G00080)" and the gene for an "uncharacterized protein (AT3G20340)", were identified to be AtLBR-2-dependent down-regulated genes (Fig. 2-1B).

Table 2-4. AtLBR-2-dependent up-regulated 65 genes after pLPS treatment.

Accession	Description	Log_2FC	Ref.
AT2G14610	**Pathogenesis-related protein 1 (PR1)***	**-5.493297**	**[42]**
AT3G23120	Receptor like protein 38 (RLP38)*	-4.553003	[43]
AT3G21500	1-deoxy-D-xylulose 5-phosphate synthase 1 (DXPS1)	-4.454822	—
AT2G30770	Putative cytochrome P450 (CYP71A13)*	-3.876201	[44]
AT1G61800	Glucose-6-phosphate/phosphate transporter 2 (GPT2)*	-3.440655	[45, 46]
AT1G21320	Nucleotide binding protein	-3.423526	—
AT2G14560	**Late upregulated in response to *Hyaloperonospora parasitica* 1 (LURP1)***	**-3.420434**	**[47]**
AT4G35180	LYS/HIS transporter 7 (LHT7)*	-3.326263	[43, 46]
AT2G29350	Senescence-associated gene 13 (SAG13)*	-3.152003	[48]
AT4G04510	Cysteine-rich receptor-like kinase (RLK) 38 (CRK38)*	-3.124063	[49]

AT2G24850	**Tyrosine aminotransferase 3 (TAT3)***	**-2.935669**	**[50]**
AT2G18660	Plant natriuretic peptide A (PNP-A)*	-2.824188	[51]
AT5G24200	Alpha/beta-Hydrolases superfamily protein*	-2.675765	[52]
AT2G04070	Multidrug and Toxin Extrusion (MATE) efflux family protein	-2.651088	—
AT3G22235	Pathogen and circadian controlled 1 (PCC1)	-2.612637	—
AT4G12470	**Azelaic acid induced 1 (AZI1)***	**-2.593354**	**[53]**
AT1G33960	avrRpt2-induced gene 1 (AIG1)*	-2.454032	[54]
AT1G65500	Uncharacterized protein	-2.423526	[45]
AT4G22470	Lipid transfer protein (LTP) family protein*	-2.414268	[55]
AT4G12490	Lipid transfer protein*	-2.37707	[56]
AT4G12480	Early Arabidopsis aluminum induced 1 (pEARLI 1)*	-2.334243	[57]
AT5G46050	**Peptide transporter 3 (PTR3)***	**-2.322650**	**[58]**
AT3G28580	P-loop containing nucleoside triphosphate hydrolases superfamily protein	-2.314015	—
AT3G50480	**Homolog of RPW8 4 (HR4)***	**-2.311148**	**[50]**
AT2G26400	Acireductone dioxygenase 3 (ARD3)	-2.302582	—
AT1G51820	Leucine-rich repeat protein kinase family protein*	-2.288417	[59]
AT1G02920	Glutathione S-transferase 7 (GSTF7)*	-2.267427	[60]
AT1G65481	Uncharacterized protein	-2.255667	—
AT1G43910	P-loop containing nucleoside triphosphate hydrolases superfamily protein*	-2.252226	[43]
AT4G17660	Protein kinase superfamily protein	-2.126580	—
AT4G26200	1-Amino-cyclopropane-1-carboxylate synthase (ACS7)	-2.091110	—
AT3G63380	Auto-inhibited Ca^{2+}-ATPase 12 (ACA12)*	-2.063108	[43, 61]
AT5G09470	Dicarboxylate carriers 3 (DIC3)	-2.058293	—
AT4G12735	Uncharacterized protein	-2.022097	—
AT2G25470	Receptor like protein 21 (RLP21)	-2.002310	—
AT3G26210	Putative cytochrome P450 (CYP71B23)	-1.987360	—
AT4G23130	**Cysteine-rich RLK 5 (CRK5)***	**-1.985073**	**[62]**
AT2G25510	**Uncharacterized protein***	**-1.984502**	**[50]**
AT5G03350	**Legume lectin family protein***	**-1.980512**	**[50]**
AT3G50770	Calmodulin-like 41 (CLM41)*	-1.936221	[56]
AT4G37990	**Elicitor-activated gene 3-2 (ELI3-2)***	**-1.895395**	**[63]**
AT4G00170	Plant vesicle-associated membrane protein (VAMP) family protein	-1.809448	—
AT2G19190	**Flg22-induced RLK 1 (FRK1)***	**-1.804904**	**[64]**

AT2G20720	Pentatricopeptide repeat (PPR) superfamily protein	-1.790359	—
AT5G44390	FAD-binding Berberine family protein	-1.785875	—
AT1G35230	Arabinogalactan-protein 5 (AGP5)*	-1.779422	[65]
AT5G53870	Early nodulin-like protein 1 (ENODL1)	-1.774478	—
AT2G04050	Multidrug and Toxin Extrusion (MATE) efflux family protein	-1.766112	—
AT1G02930	**Glutathione S-transferase 6 (GSTF6)***	**-1.750494**	**[66]**
AT2G43620	Chitinase family protein*	-1.717382	[67]
AT1G21250	**Cell wall-associated kinase 1 (WAK1)***	**-1.706512**	**[50, 68]**
AT1G80130	Tetratricopeptide repeat (TPR)-like superfamily protein*	-1.679920	[69]
AT5G44575	Uncharacterized protein	-1.671623	—
AT5G62480	Glutathione S-transferase TAU 9 (GSTU9)	-1.630394	—
AT5G10760	Apoplastic, EDS1-dependent 1 (AED1)*	-1.621488	[51]
AT5G24640	Uncharacterized protein	-1.616614	—
AT5G64000	3'(2'),5'-bisphosphate nucleotidase (SAL2)	-1.600337	—
AT3G28540	P-loop containing nucleoside triphosphate hydrolases superfamily protein	-1.584674	—
AT1G05730	Uncharacterized protein (DUF842)	-1.542038	—
AT1G26420	FAD-binding Berberine family protein	-1.526992	[70]
AT1G67520	Lectin protein kinase family protein	-1.478748	—
AT2G26440	Pectin methylesterase 12 (PME12)*	-1.460767	[71]
AT3G26830	Phytoalexin deficient 3 (PAD3)*	-1.409278	[72, 73]
AT2G41730	Uncharacterized protein	-1.405069	—
AT1G15520	**Pleiotropic drug resistance 12 (PDR12)***	**-1.361787**	**[74]**

Genes up-regulated in an AtLBR-2-dependent manner after 24 h pLPS treatment were identified (FDR < 0.01, Log_2FC < -1.35). Genes, which were related to plant–pathogen interaction or to SA, are indicated by asterisks or in bold type, respectively, with references.

AtLBR-2 is indispensable for pLPS-induced defense-related GO terms.

To determine the importance of the 65 AtLBR-2-dependent up-regulated genes in the GO classification of 605 up-regulated genes, I performed GO analysis for 540 genes, excluding the above-mentioned 65 genes from the 605 up-regulated genes ($P < 0.01$, Fig. 2-2, red line) (Table 2-1). Comparing the results of the GO analysis revealed that 540 genes showed no enrichment for defense-related GO terms, including responses to bacterium, SA stimulus, ABA stimulus, wounding, and drug. These results highlight the importance of 65 genes in defense-related GO terms, and demonstrate that AtLBR-2 might be indispensable for the expression of pLPS-induced defense-related genes.

Characterization of 65 AtLBR-2-dependent up-regulated genes.

The details of the 65 pLPS-induced AtLBR-2-dependent up-regulated genes are shown in Table 2-4. I expected that *PR1* would be one of the 65 AtLBR-2-dependent up-regulated genes, because I previously reported that *atlbr* mutants showed deficiencies in the expression of pLPS-induced *PR1* (AT2G14610) [40]. Consistent with my prediction, as shown in Table 2-4, *PR1* was the most differentially-expressed gene among the AtLBR-2-dependent up-regulated genes. Furthermore, most of the 65 genes have been reported to be associated with plant–pathogen interaction and with SA-regulated responses.

These 65 genes were also annotated to each of the three GO categories; CC, molecular function (MF), and BP. These genes were assigned the CC GO terms, “endomembrane system” (27.1%), “membrane” (17.1%), and “membrane-bound organelle” (11.4%; Table 2-5). Thus, approximately 50% of these genes were categorized as membrane-related CC GO terms, highlighting the inter-relationship between the proteins encoded by these genes and AtLBR-2 [40]. Furthermore, the MF GO terms related to catalytic (44.1%), binding (35.3%), and transporter (11.8%) activities were mostly enriched. They were also predicted to participate in 25 BP GO terms, mainly in the “response to stress” (12.0%), “cellular metabolic process” (10.6%), “response to biotic stimulus” (9.2%), and in “response to other organisms” (9.1%). Thus, interestingly, approximately 50% of these genes were involved in response to stress and stimuli. To further define the functions of these 65 genes, the enriched pathways were identified by KOBAS (Table 2-6). The pathway analysis also revealed that the 65 genes were involved in defense-related pathways, including “camalexin biosynthesis”, “glutathione-mediated detoxification II”, and “plant–pathogen interaction”.

Table 2-5. GO-term-enriched tables of AtLBR-2-dependent up-regulated 65 genes.

CC GO term	%
Endomembrane system	27.1
Membrane	17.1
Intercellular part	14.3
Membrane-bound organelle	11.4
Intercellular organelle	11.4
External encapsulation structure	8.6
Apoplast	4.3
Membrane part	1.4
Intercellular organelle part	1.4
Organelle membrane	1.4

MF GO term	%
Catalytic activety	44.1
Binding	35.3
Transporter activety	11.8
Electron carrier activety	5.9
Structual molecule activety	1.5

BP GO term	%
Response to stress*	12.0
Cellular metabolic process	10.6
Response to chemical stimulus*	9.9
Response to biotic stimulus*	9.2
Response to other organism*	9.1
Primary metabolic process	6.3
Transport	5.6
Response to endogeneous stimulus*	4.2
Secondary metabolic process	4.2
Biosynthetic process	4.2
Macromolecule metabolic process	3.5
Immune response*	2.8
Nitrogen compound metabolic process	2.8
Response to abiotic stimulus*	2.1
Regulation of biological process	2.1
Transmembrane transport	2.1
Catabolic process	2.1
Small molecule metabolic process	1.4
Oxidation-reduction process	0.7
Aging	0.7
Establishment of localization in cell	0.7
Multicallular organism reproduction process	0.7
Cell wall organization or biogengesis	0.7
Cellular response to stimulus*	0.7
Cell death	0.7

The 65 AtLBR-2-dependent up-regulated genes were classified by functional categories under the following GO terms: CC (level 2), MF (level 1), and BP (level 2) using the VirtualPlant 1.3 web service. BP GO terms related to stress and stimulus are indicated by asterisks.

Table 2-6. Pathway enrichment analysis of 65 AtLBR-2-dependent up-regulated genes.

Term	Pathway Database	Database ID	IN	BN	*P*-Value
Camalexin biosynthesis	BioCyc	CAMALEXIN-SYN	3	32	7.44E-05
Glutathione-mediated detoxification II	BioCyc	PWY-6842	3	50	0.000258
Glutathione metabolism	KEGG	ath00480	3	93	0.001468
Cysteine and methionine metabolism	KEGG	ath00270	3	112	0.002458
Plant-pathogen interaction	KEGG	ath04626	3	167	0.007317

A *P*-Value < 0.01 was used as a threshold to select significant pathways. IN; Input number, BN; Background number.

***atlbr-2-1* mutants showed defect in up-regulation of six pLPS-induced genes.**

To confirm the RNA-Seq results of AtLBR-2-dependent up-regulated genes, I assigned and tested several genes involved in plant–pathogen interaction by RT-PCR (Fig. 2-3). In all of the tested 6 genes, putative cytochrome P450 (*CYP71A13*), late upregulated in response to *Hyaloperonospora parasitica* (*LURP1*), plant natriuretic peptide A (*PNP-A*), avrRpt2-induced gene 1 (*AIG1*), glutathione S-transferase 7 (*GSTF7*), and pleiotropic drug resistance 12 (*PDR12*), I could detect the significant differences between WT and the *atlbr-2-1* at 24 h of pLPS treatments, indicating that AtLBR-2-dependent up-regulated genes identified by RNA-Seq were also confirmed by qRT-PCR. However, the expression levels of these 6 genes were not completely abolished in pLPS-treated *atlbr-2-1* mutants. These results

suggested the possibility that *AtLBR-1*, the paralog of *AtLBR-2*, may compensate for the absence of the *AtLBR-2* gene. Therefore, I conducted qRT-PCR analysis for these 6 genes with the *atlbr-1* mutant seedlings by the same method that was used on the *atlbr-2-1* mutant (Fig. 2-4) [40]. Similar to the results shown in Fig. 2-3, I detected significant differences in all tested genes in pLPS-treated WT and *atlbr-1* mutants, suggesting that AtLBR-1 might also play an important role in some AtLBR-2-dependent up-regulated genes. Furthermore, to exclude the possibility of contamination by other bacterial components, we purified the commercial pLPS. Seedlings were treated with purified pLPS and were analyzed by qRT-PCR (Fig. 2-5). Similar to the results shown in Fig. 2-3, I could detect the significant differences between WT and *atlbr-2-1* in all of the genes tested at 24 h of purified pLPS treatments, confirming that this phenomenon was not caused by contamination.

Although I did not observe read counts from the region downstream of the T-DNA insertion site of *AtLBR-2* (Fig. 2-6), the possibility of slight expression of AtLBR-2 is not excluded because the T-DNA insertion site of the *atlbr-2-1* is located just next to the stop codon of the gene. Thereafter, I conducted qRT-PCR using the cDNA obtained from another pLPS-treated T-DNA insertion line, *atlbr-2-2* [40]. Similar to that in the *atlbr-2-1*, I could detect the significant differences between pLPS-treated WT and the *atlbr-2-2* (Fig. 2-7).

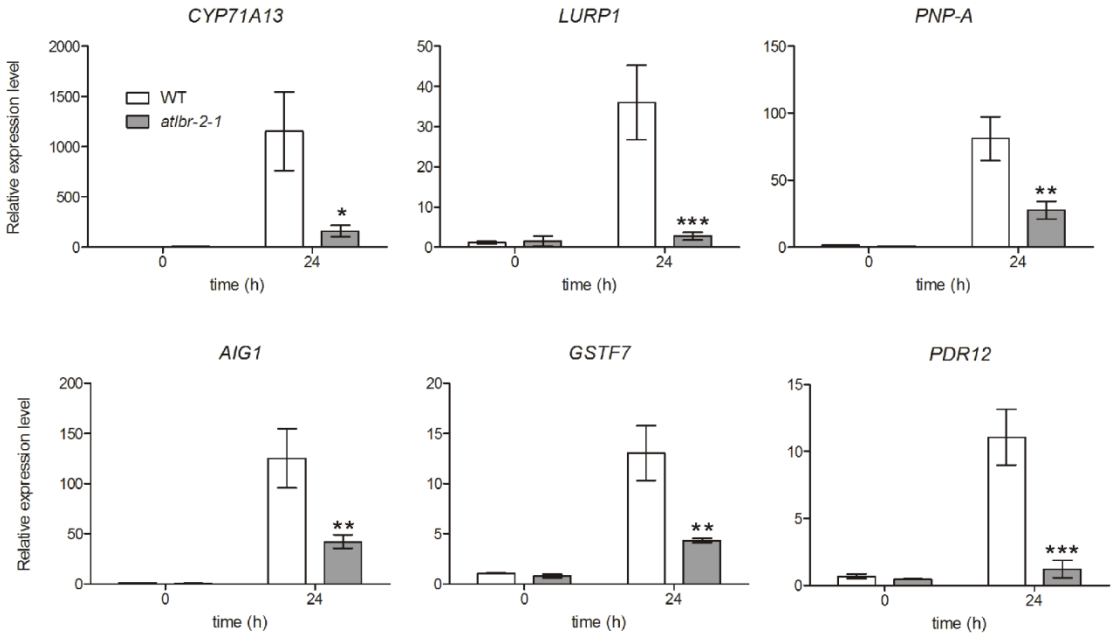

Figure 2-3. qRT-PCR analysis of six AtLBR-2-dependent up-regulated genes.

Among the 65 pLPS-induced AtLBR-2-dependent up-regulated genes, 6 defense-related genes (*CYP71A13*, *LURP1*, *PNP-A*, *AIG1*, *GSTF7*, and *PDR12*) were randomly selected and analyzed by qRT-PCR in WT and *atlbr-2-1* plants treated with pLPS. The mean expression values were calculated from the results of three independent experiments. Means ± standard errors are presented. Significant differences among the means were determined by two-way ANOVA followed by *post hoc* Bonferroni test compared to WT plants; **P* < 0.05, ***P* < 0.01, ****P* < 0.001.

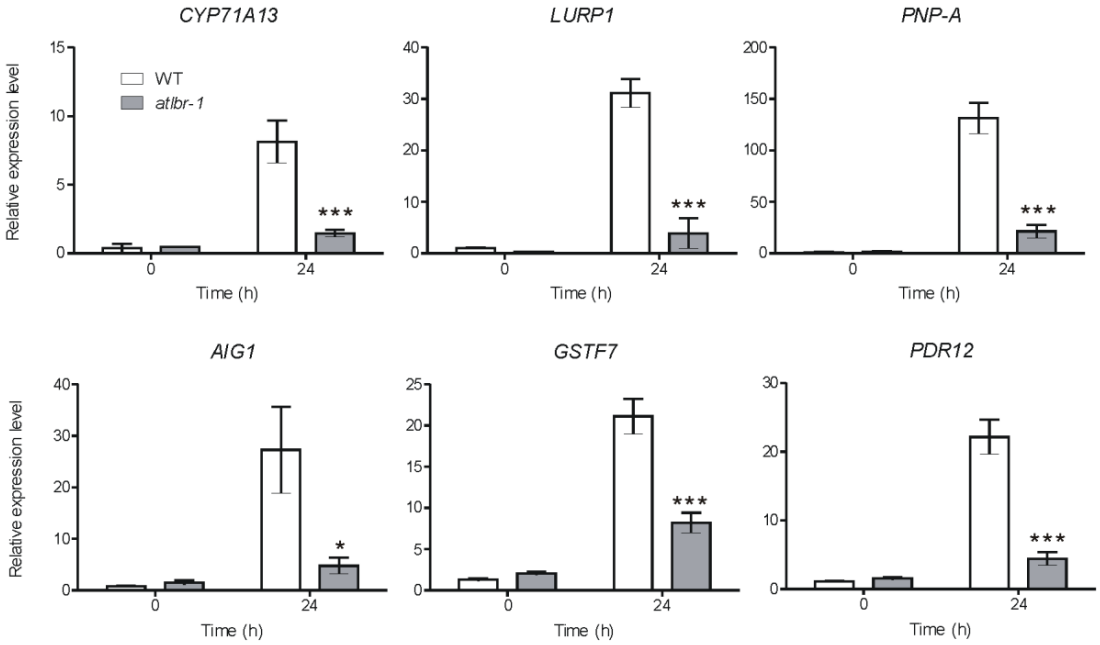

Figure 2-4. mRNA levels of 6 AtLBR-2-dependent up-regulated genes in the pLPS-treated *atlbr-1*.

The seedlings having a mutation in *AtLBR-1*, a paralog of *AtLBR-2*, were treated with pLPS by the same method described in the Methods section. cDNA obtained from them were analyzed by qRT-PCR. The mean expression values were calculated from the results of three independent experiments. Means ± standard errors are presented. Significant differences among the means were determined by two-way ANOVA followed by *post hoc* Bonferroni test compared to WT plants; **P* < 0.05, ****P* < 0.001.

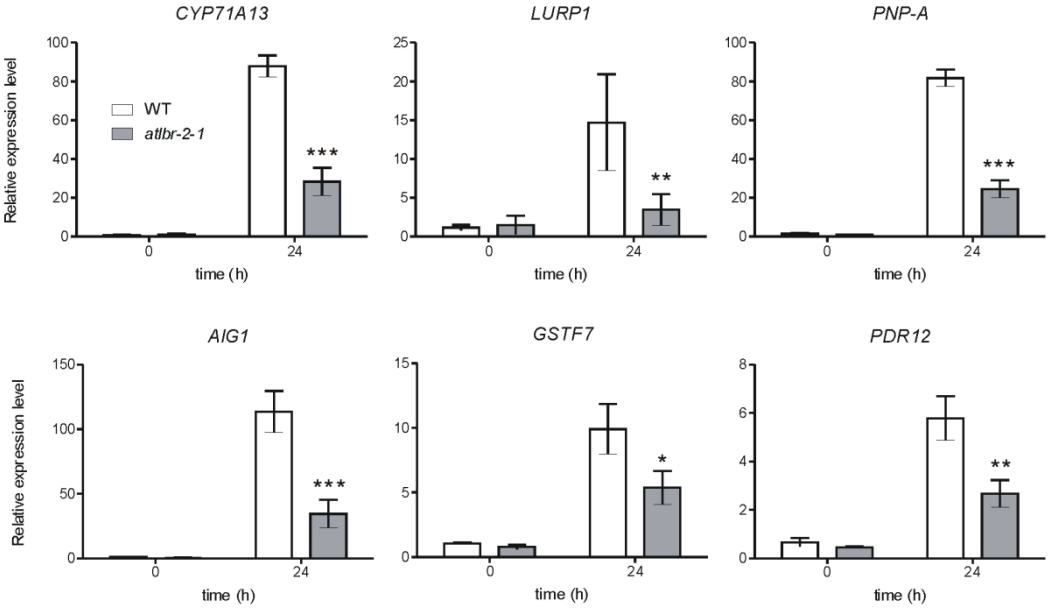

Figure 2-5. mRNA levels of 6 AtLBR-2-dependent up-regulated genes in seedlings treated with purified pLPS.

Purchased pLPS was purified by degradation of nucleic acids and proteins with DNase I, RNase, and proteinase K. mRNA levels of 6 AtLBR-2-dependent up-regulated genes in WT and *atlbr-2-1* seedlings treated with 100 μg/ml purified pLPS during 24 h were detected by qRT-PCR. The mean expression values were calculated from the results of three independent experiments. Means ± standard errors are presented. Significant differences among the means were determined by two-way ANOVA followed by *post hoc* Bonferroni test compared to WT plants; **P* < 0.05, ***P* < 0.01, ****P* < 0.001.

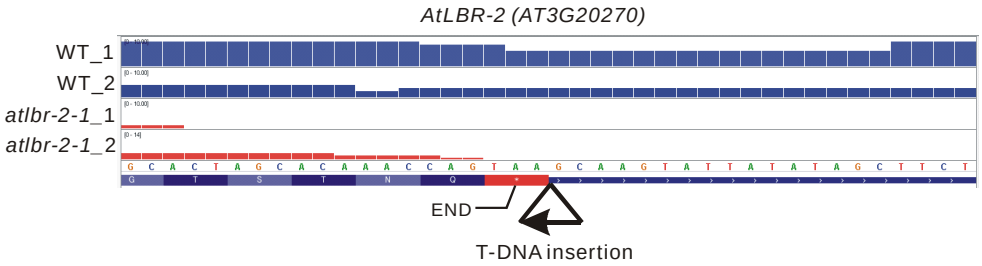

Figure 2-6. T-DNA insertion effect on the *atlbr-2-1*.

Data of RNA-Seq reads from the *atlbr-2-1* T-DNA insertion region were visualized by Integrative Genomics Viewer (IGV).

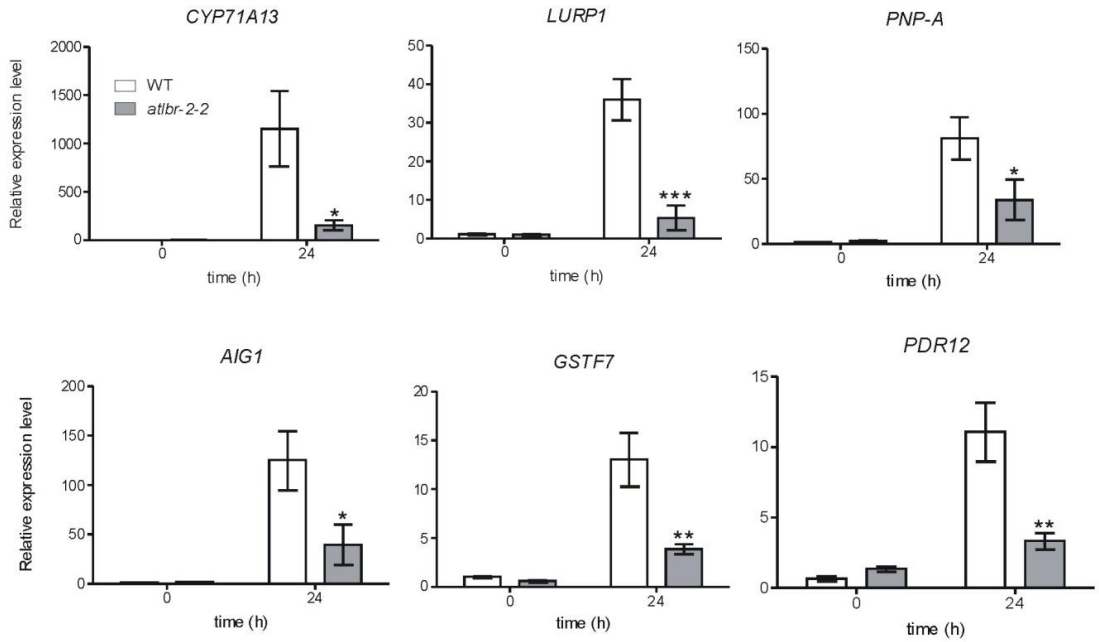

Figure 2-7. mRNA levels of 6 AtLBR-2-dependent up-regulated genes in the pLPS-treated *atlbr-2-2*.

To confirm the RNA-Seq results, cDNA obtained from pLPS-treated or untreated WT and *atlbr-2-2* plants, another T-DNA insertion line of *AtLBR-2*, were analyzed by qRT-PCR. The mean expression values were calculated from the results of three independent experiments. Means ± standard errors are presented. Significant differences among the means were determined by two-way ANOVA followed by *post hoc* Bonferroni test, and compared to WT plants; **P* < 0.05, ***P* < 0.01, ****P* < 0.001.

Validation of RNA-Seq data by qRT-PCR.

To validate RNA-Seq results, I conducted the expression analysis by qRT-PCR for randomly selected pLPS-responsive genes, including AtLBR-2-dependent or -independent up- or down-regulated genes. Fig. 2-8 shows a comparison between the results from qRT-PCR and RNA-Seq analysis. For all 20 tested genes, transcript levels determined by qRT-PCR analysis were similar to those detected using RNA-Seq, indicating the reliability of the RNA-Seq data.

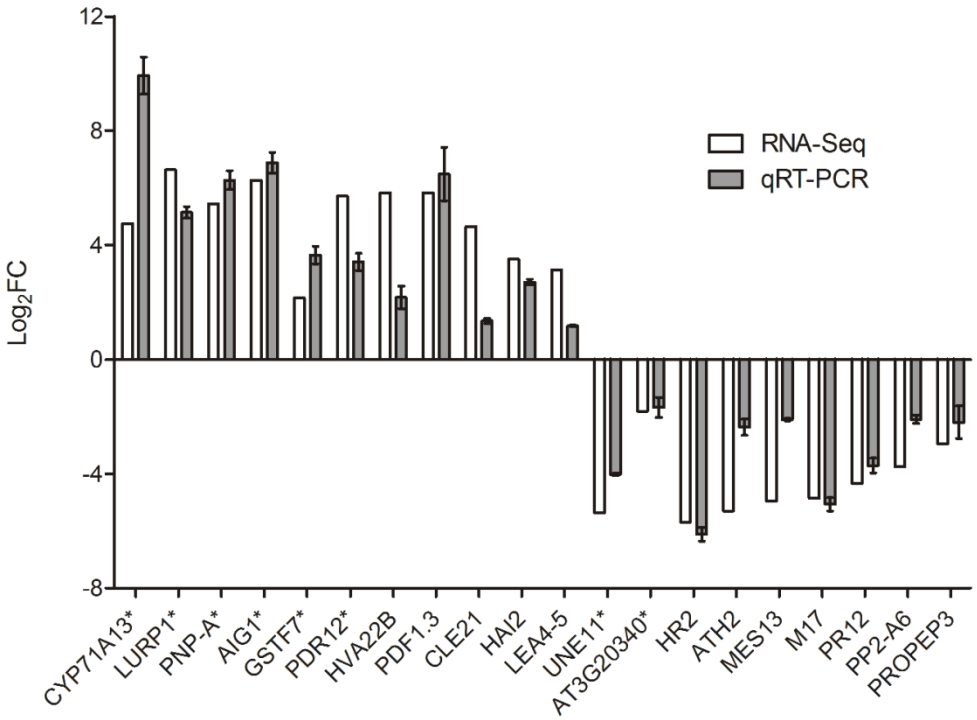

Figure 2-8. Comparison of RNA-Seq results with those of qRT-PCR.

The Log_2FC values for transcript levels observed in RNA-Seq data (white bar) of randomly selected 20 genes, including AtLBR-2-dependent -independent up- or down-regulated genes, were compared to the results obtained from qRT-PCR (gray bar). AtLBR-2-dependent up- or down-regulated genes are indicated with asterisk: *CYP71A13*, *LURP1*, *PNP-A*, *AIG1*, *GSTF7*, *PDR12*, *UNE11*, and AT3G20340. AtLBR-2-independent up- or down-regulated genes are indicated without asterisk: *HVA22B* (AT5G62490), HVA22 homologue B; *PDF1.3* (AT2G26010), plant defensin 1.3; *CLE21* (AT5G64800), clavata3/ESR-related 21; *HAI2* (AT1G07430), highly ABA-induced 2; *LEA4-5* (AT5G06760), late embryogenesis abundant 4-5; *HR2* (AT3G50460), homolog of RPW8 2; *ATH2* (AT3G47740), A. thaliana ABC2 homolog 2; *MES13* (AT1G26360), methyl esterase 13; *M17* (AT2G41260), late embryogenesis abundant gene; *PR12* (AT1G75830); *PP2-A6* (AT5G45080), phloem protein 2-A6; *PROPEP3* (AT5G64905), elicitor peptide 3 precursor.

A proposed pathway: AtLBR-2-mediated SAG accumulation and following SA-related gene expression.

In the WT, pLPS treatment induced differential expression of many genes related to SA, a potent inducer of pathogen-induced defense responses (Table 2-7). Among these, 14 genes were identified as AtLBR-2-dependent up-regulated genes. In addition, 65 AtLBR-2-dependent up-regulated genes were responsible for the enrichment of GO term "response to SA stimulus" (Fig. 2-2). These RNA-Seq data analyses suggested the association of AtLBR-2 with pLPS-induced SA signaling. Therefore, first, I investigated whether pLPS-induced SA accumulation levels were altered in *atlbr-2-1* plants. Treatment of both WT and the *atlbr-2-1* with pLPS did not result in significant changes in the content of free SA (Fig. 2-9A, left panel). In contrast, the accumulation levels of conjugated SA glucoside (SAG) between WT and the *atlbr-2-1* showed significant differences at 8 h after pLPS treatment (Fig. 2-9A, right panel). These results indicated that AtLBR-2 has an important role in pLPS-induced SAG accumulation. Furthermore, to confirm the relationship between AtLBR-2-mediated SAG accumulation and SA-related gene expression, I investigated the expression levels of 3 AtLBR-2-dependent up-regulated genes, *PR1*, *LURP1*, and *PDR12*, in SA-treated WT plants and *atlbr-2-1* mutants by qRT-PCR. These 3 genes are known as SA-related genes, and *atlbr-2-1* mutants showed significant differences in the expression of

these genes after pLPS treatment ([40] and Fig. 2-3). As shown in Fig. 2-9B, I observed the up-regulation of all tested genes in the SA-treated *atlbr-2-1* to be at the same level, as or more, than that of WT plants. These results suggested that AtLBR-2 may act upstream of the SA signaling (SAG accumulation) pathway induced by pLPS treatment.

Table 2-7. Up- or down-regulation of SA-related genes in pLPS-treated WT plants.

I investigated the differential expression of 44 SA-related genes that had been reported previously. Among them, 25 genes were up-regulated (FDR < 0.01, Log_2FC > 1.35) and 19 genes were down-regulated (FDR < 0.01, Log_2FC < -1.35) in pLPS-treated WT plants. The genes identified as AtLBR-2-dependent up-regulated genes are indicated by asterisks.

Accession	Gene	Description	Log_2FC	Ref.
AT2G14610	PR1*	Pathogenesis-related protein 1	7.8961	[42]
AT2G14560	LURP1*	Late upregulated in response to *Hyaloperonospora parasitica*	6.6324	[47]
AT5G54610	ANK	Ankyrin-repeat transmembrane protein BDA1	5.7663	[50, 68]
AT1G15520	PDR12*	Pleiotropic drug resistance 12	5.7092	[74]
AT4G37990	ELI3-2*	Elicitor-activated gene 3-2	5.6854	[63]
AT1G12940	NRT2.5	Nitrate transporter 2.5	5.6152	[50]
AT5G46350	WRKY8	WRKY DNA-binding protein 8	4.7893	[75]
AT5G13320	PBS3	4-substituted benzoates-glutamate ligase GH3.12	4.0142	[76]
AT2G19190	FRK1*	Flg22-induced RLK 1	3.8554	[64]
AT1G21250	WAK1*	Wall-associated receptor kinase 1	3.8309	[50, 68]
AT4G14400	ACD6	Accelerated cell death 6	3.7815	[50]
AT2G24850	TAT3*	Tyrosine aminotransferase 3	3.4777	[50]
AT1G48000	MYB112	Putative transcription factor MYB112	3.4516	TAIR
AT4G12470	AZI1*	Azelaic acid induced 1	3.1286	[53]
AT2G25510	AT2G25510*	Uncharacterized protein	3.0497	[50]
AT5G03350	AT5G03350*	Legume lectin family protein	2.7349	[50]

AT4G23130	CRK5*	Cysteine-rich RLK 5	2.6755	[62]
AT3G50480	HR4*	Homolog of RPW8 4	2.2874	[50]
AT1G02930	GSTF6*	Glutathione S-transferase 6	1.8091	[66]
AT4G23210	CRK13	Cysteine-rich RLK 13	1.7417	[77]
AT4G23170	CRK9	Cysteine-rich RLK 9	1.6418	[68]
AT5G54240	CNGC4	Cyclic nucleotide-gated ion channel 4	1.5442	[50]
AT5G46050	PTR3*	Peptide transporter 3	1.5297	[58]
AT1G21270	WAK2	Wall-associated receptor kinase 2	1.5260	TAIR
AT3G09010	AT3G09010	Protein kinase superfamily protein	1.4225	[50]
AT1G17980	PAPS1	Poly(A) polymerase 1	-1.3765	[78]
AT2G47730	GSTF8	Glutathione S-transferase PHI 8	-1.4073	[50]
AT4G23810	WRKY53	WRKY DNA-binding protein 53	-1.4345	[79]
AT3G11340	UGT76B1	UDP-dependent glycosyltransferase 76B1	-1.5205	[50]
AT5G45110	NPR3	NPR1-like protein 3	-1.7294	[80]
AT1G28380	NSL1	Protein necrotic spotted lesions 1	-1.7437	[81]
AT3G25190	AT3G25190	Vacuolar iron transporter homolog 2.1	-1.7665	[50]
AT4G13510	AMT1	Ammonium transporter 1;1	-1.9057	[50]
AT3G01420	DOX1	Alpha-dioxygenase	-1.9216	[50, 68]
AT1G29690	CAD1	Protein constitutively activated cell death 1	-1.9219	[82]
AT5G62470	MYB96	Putative transcription factor MYB96	-1.9701	[83]
AT3G20600	NDR1	Non race-specific disease resistance 1	-2.1589	[84]
AT4G31800	WRKY18	WRKY DNA-binding protein 18	-2.5420	[50, 79, 85]
AT1G80840	WRKY40	WRKY DNA-binding protein 40	-2.9525	[85]
AT3G24500	MBF1C	Multiprotein-bridging factor 1c	-3.3486	[86]
AT2G40000	HSPRO2	HS1 PRO-1 2-like protein	-3.4538	[87]
AT1G07400	HSP17.8-CI	Class I heat shock protein	-3.4960	[50]
AT5G22570	WRKY38	WRKY DNA-binding protein 38	-3.7252	[50, 79]
AT4G25560	MYB18	Putative transcription factor MYB18	-6.6379	TAIR

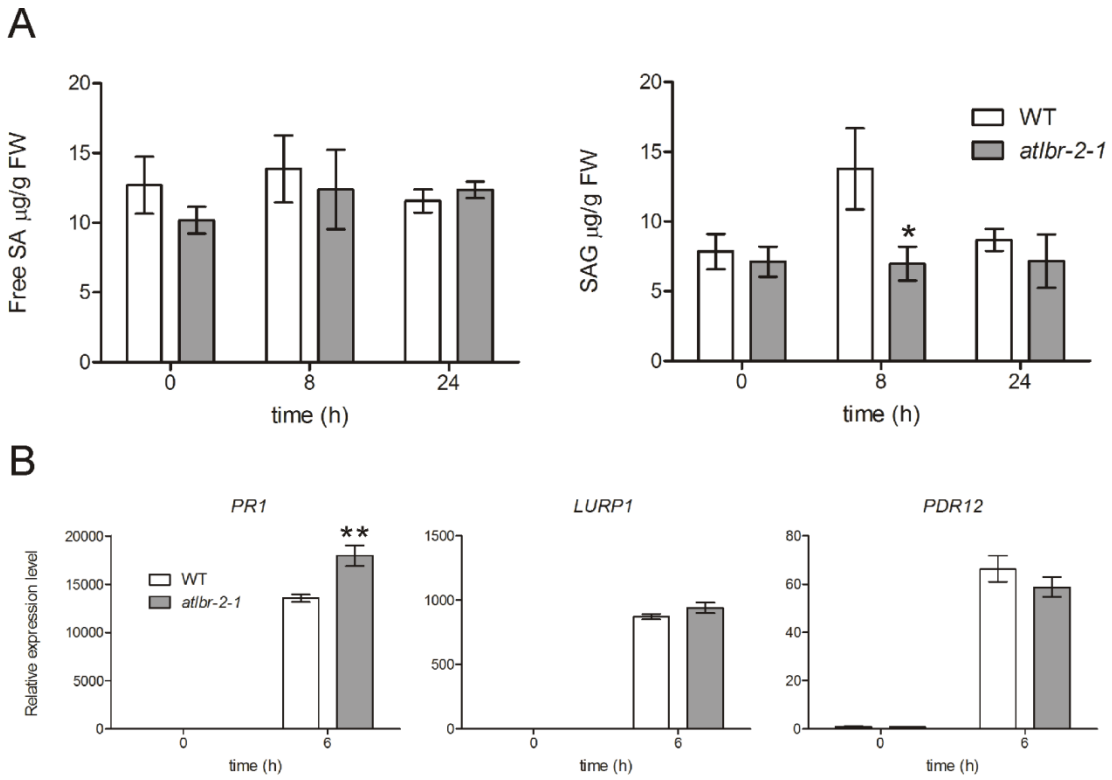

Figure 2-8. pLPS-induced free SA and SAG accumulation and SA-induced gene expression.

(**A**) Quantification of the total levels of free SA and SAG were measured by HPLC using samples extracted from *Arabidopsis* treated with pLPS for the indicated time. (**B**) Among the 65 pLPS-induced AtLBR-2-dependent up-regulated genes, the expression of the 3 SA-related genes (*PR1*, *LURP1*, and *PDR12*) were analyzed by qRT-PCR in WT and the *atlbr-2-1* mutants plants treated with SA. The mean values were calculated from the results of three independent experiments. Means ± standard errors are presented. Significant differences among the means were determined by two-way ANOVA followed by *post hoc* Bonferroni test compared to WT plants; **P* < 0.05, ***P* < 0.01. FW, fresh weight.

Discussion

My primary interest in this Chapter 2 was in understanding the role of AtLBR-2 in LPS-induced plant defense responses. In the Chapter 1 study, I concluded that apoplast-localized AtLBR-2 might play an important role in binding and transferring LPS to the LPS receptor. However, the functional properties of AtLBR-2 have not been characterized in detail. Therefore, in this Chapter 2 study, I analyzed, for the first time, the effect of AtLBR-2 on transcriptional changes involved in pLPS treatment using RNA-Seq technology. By my RNA-Seq analysis, I identified that pLPS-induced up-regulated genes were associated with defense-related, as well as metabolism-related processes, which is consistent with a previous study that used LPS from *B. cepacia* [41]. Furthermore, I found a strong association between AtLBR-2 and SA by my RNA-Seq analysis and, in fact, I demonstrated the reduced level of pLPS-induced SAG accumulation in the *atlbr-2-1*, and the SA-induced normal gene expression in *atlbr-2-1* mutants. My data revealed the importance of AtLBR-2 in SA-mediating signaling pathway in response to LPS or when triggered by LPS.

AtLBR-2 and SA signaling

In this study, I identified 65 AtLBR-2-dependent genes that were up-regulated after pLPS treatment. The pathway analysis of these 65 genes revealed a significant enrichment of

defense-related pathways. In fact, 44 of these genes encode proteins related to defense responses, and 14 genes, including *PR1*, *LURP1*, tyrosine aminotransferase 3 (*TAT3*), azelaic acid induced 1 (*AZI1*), peptide transporter 3 (*PTR3*), homolog of RPW8 4 (*HR4*), cysteine-rich receptor-like kinase (RLK) 5 (*CRK5*), elicitor-activated gene 3-2 (*ELI3-2*), flg22-induced RLK 1 (*FRK1*), glutathione S-transferase 6 (*GSTF6*), cell wall-associated kinase 1 (*WAK1*), *PDR12*, AT2G25510, and AT5G03350, are known to be induced by SA (Table 2-7). The SA signaling is mediated by at least two mechanisms, one requiring the NPR1 and the second, which is independent of NPR1 [32]. *PR1* is well known as a marker for NPR1-dependent SA-induced pathway. In addition, Blanco *et al.* identified some NPR1-dependent SA-induced genes, including *HR4*, *WAK1*, and AT5G03350 by microarray analysis in SA-treated WT and *npr1-1* plants [50]. Furthermore, they also identified NPR1-independent SA-induced genes, including *TAT3* and AT2G25510. These facts, along with my findings in this study, suggested the possibility that AtLBR-2 plays an important role in both NPR1-dependent and -independent signaling pathways triggered by LPS. Furthermore, I demonstrated that LPS-induced SAG accumulation was dependent on AtLBR-2. The LPS-induced accumulation of SAG, but not of SA, has been observed in previous studies, and might cause the transient production of SA and the stable accumulation of SAG [88]. In addition, the SA-treated *atlbr-2-1* showed up-regulation of SA-related genes

at levels similar to or more than those exhibited by WT plants. These results as well as my previous findings support the hypothesis that AtLBR-2 binds to LPS directly in the apoplastic region of *Arabidopsis* and, subsequently, induces the accumulation of SA (or SAG), leading to the activation of both NPR1-dependent and -independent signaling pathways and the gene expression that follows them [40].

Interestingly, *NPR1* expression appeared to be up-regulated after inoculation with *P. syringae* pv. *tomato* (*Pst*) DC3000 or upon SA treatment [89, 90]; however, no difference was observed between the untreated and pLPS-treated WT plants in the present study (FDR < 0.01). The WRKY transcription factors, including WRKY18, WRKY38, and WRKY53, reported to be the targets of NPR1 during SAR [57], appear to be down-regulated in the pLPS-treated WT plants (Table 2-7). Shah suggested the existence of a negative feedback loop involving NPR1, which regulates the accumulation of SA [32]. Moreover, in the present study, I showed that SAG concentration returned to the basal levels after 24 h of pLPS treatment. Therefore, based on these observations, I speculated that long-term treatment of pLPS (24 h) might induce SA negative feedback loop involving *NPR1* suppression and result in a decline in SA (SAG) to basal levels.

AtLBR-2 and camalexin

The 65 AtLBR-2-dependent up-regulated genes included *CYP71A13* and phytoalexin deficient 3 (*PAD3*). These genes encode cytochrome P450 enzymes, which contribute to the enrichment of the "camalexin biosynthesis" pathway. Camalexin is an indole alkaloid phytoalexin produced by *Arabidopsis* that is thought to be important for resistance to necrotrophic fungal pathogens. A previous study revealed the LPS-induced camalexin production in plants [91]. CYP71A13 catalyzes the conversion of indole acetaldoxime to indole-3-acetonitrile, an intermediate in the camalexin biosynthesis [72]. PAD3 catalyzes the conversion of dihydrocamalexic acid to camalexin, which is the last step of camalexin biosynthesis [44]. Interestingly, Nafisi *et al*. demonstrated that the expression levels of *CYP71A13* and *PAD3* were coregulated in response to infection by *P. syringae* [72]. Furthermore, SA is required for camalexin synthesis, which is mediated by an NPR1-independent pathway [92, 93]. These findings from previous research and the RNA-Seq analysis performed in this study led to the hypothesis that the binding and transfer of LPS to LPS receptor by AtLBR-2 and further SA (SAG) induction might be necessary to activate efficient LPS-induced camalexin biosynthesis. More research is needed to better understand the relationship between AtLBR-2 and camalexin biosynthesis in *Arabidopsis*.

AtLBR-2 and ATPase

Four genes (AT1G43910, AT3G28540, AT3G28580, and AT3G63380) encoding proteins that function as an ATPase were also among the 65 AtLBR-2-dependent up-regulated genes. Relationship between the four genes and their defense responses have been reported previously. AT1G43910 and AT3G28540 were consistently higher in *sni1*, a transcription repressor of NPR1, when compared with the WT plants [94]. AT3G28580 has been used as singlet oxygen ($^1O_2$)-responsive gene [95, 96]. $^1O_2$ is a singular ROS that can be produced by phytotoxins during plant–pathogen interactions [97]. In addition, Frei dit Frey showed that AT3G63380 (auto-inhibited Ca^{2+}-ATPase 12) cannot interact with FLS2, the bacterial flagellin peptide flg22 receptor, but might contribute to the control of cytosolic Ca^{2+} levels during flg22 responses [61]. Furthermore, a previous report described the relationship between the plasma membrane ATPase of plants and PAMPs-induced rapid extracellular alkalinization [98]. These reports lead us to speculate that AtLBR-2 might be related to LPS-induced ATPase-related responses, e.g. extracellular alkalinization and Ca^{2+} influx/efflux.

AtLBR-2 and protein kinases

For understanding the LPS recognition mechanism(s), it is essential to investigate the LPS receptor that binds to LPS and initiates a signaling cascade inside the cell via its kinase

activity. The well known PAMPs, including flg22, bacterial elongation factor Tu (EF-Tu) peptide elf18, and fungal cell wall component chitin, are recognized by pattern recognition receptors, flagellin-sensitive 2 (FLS2), EF-Tu receptor (EFR), and chitin elicitor receptor kinase 1 **(**CERK1), respectively [99]. Interestingly, the genes induced or repressed by PAMPs are clearly correlated. The flg22 treatment induced the expression not only of EFR and CERK1, in addition to that of FLS2 [100]. In this study, I identified seven AtLBR-2-dependent up-regulated genes, which encode protein kinases (*CRK5*, *CRK38*, *FRK1*, *WAK1*, AT1G51820, AT1G67520, and AT4G17660). The bulb-type lectin S-domain-1 RLK LORE (AT1G61380), which is required for sensing of LPS from *Pseudomonas* and *Xanthomonas* species [4], was not, but lectin protein kinase family protein (AT1G67520) was included in the list. AT1G67520 is known as G-type lectin RLK and is similar to LORE; however, it lacks the transmembrane region [101]. Interestingly, both flg22 and elf26 treatments induced *LORE* and AT1G67520 [100]. These results suggest that AT1G67520 might be involved in recognition of LPS or other related PAMPs. The LPS-responsive S-domain RLK (Nt-Sd-RLK) was also identified in *Nicotiana tabacum* [102]. Signal transduction via RLKs seems to be required for the activation of LPS-induced plant defense responses. I also focused on CRK5, which is potential target gene of WRKY transcription factors. Chen *et al*. reported that *CRK5* expression was up-regulated by SA treatment and

constitutive over-expression of CRK5 led to increased resistance to *Pst* DC3000, which was associated with rapidly induced expression of *PR1* after pathogen infection [103]. Moreover, I also focused on leucine-rich repeat (LRR) protein kinase family protein encoded by AT1G51820, because FLS2, EFR, and their co-receptor brassinosteroid insensitive 1 (BRI1)-associated receptor kinase 1 (BAK1) belong to the LRR-RLK family. Interestingly, AT1G51820 expression was up-regulated after infection with oomycete downy mildew pathogen [59]. These studies suggest that AtLBR-2-related protein kinases might be involved in the perception of PAMP. I speculate on possible LPS perception systems via unknown protein kinases other than LORE or those, which cooperate with LORE.

In this Chapter 2, I revealed the indispensable role of AtLBR-2 in the up-regulation of pLPS-induced genes associated with defense responses. Further experiments also suggested the existence of an SA-mediated LPS signaling system via AtLBR-2. I suggest that 65 AtLBR-2-related proteins might be the key candidate molecules in LPS-induced defense mechanisms in plants.

Materials and Methods

***Arabidopsis* growth conditions and pLPS or SA treatment.** *Arabidopsis* ecotype Col-0 was used as the WT plants in this study. All mutants were in the Col background. After 5 d of growth on MS agar plates at 22–24 °C under a 16 h light/ 8 h dark cycle, the seedlings were transferred to two separate liquid MS medium supplemented with 100 μg/ml pLPS and 200 μM SA (Wako) that were then kept under continuous light conditions for 24 h and 6 h, respectively. Untreated seedlings were used as controls (0 h). The experiments were performed in three biological replicates.

RNA sample preparation and high-throughput sequencing. After the treatment, the seedlings were powdered in liquid nitrogen and RNA was extracted using the plant total RNA extraction Miniprep system (Viogene) according to the manufacturer's instructions. The quality of total RNA obtained from pLPS-treated or untreated seedlings was evaluated using the value of RNA Integrity Number (RIN) in the Agilent Bioanalyzer 2100 (Agilent). The total RNA concentration was measured using a Qubit RNA assay kit (Thermo Fisher Scientific). The mRNAs were purified from 100 ng total RNAs by NEBNext Poly(A) mRNA Magnetic Isolation Module (New England Biolabs), according to the manufacturer's instructions. The sequencing libraries were prepared by NEBNext Ultra Directional RNA

Library Prep Kit for Illumina (New England Biolabs), according to the manufacturer's instructions. The quality of the libraries was assessed by a microchip electrophoresis system (MCE-202 MultiNA; Shimadzu) and their quantities were measured by Qubit dsDNA BR assay kit (Thermo Fisher Scientific). After equimolar amounts of the libraries were pooled, they were used for paired-end read sequencing (2 × 101 bp) on Illumina Hiseq 4000 (Illumina).

Availability of data and materials. The RNA-Seq raw data (Table 2-8) presented in this paper have been deposited in the DNA Data Bank of Japan (DDBJ) Sequence Read Archive (DRA) (http://trace.ddbj.nig.ac.jp/dra/index_e.shtml; Accession no. DRA005496).

Read mapping and transcript assembly. After the quality evaluation and removal of adapter-containing reads, more than 88% left and right reads could be mapped to the *Arabidopsis* TAIR 10 genomes using TopHat software (http://www.ccb.jhu.edu/software/tophat/) (Table 2-8) [104]. The concordant pair alignment rate was more than 86%. The transcripts were assembled and fragments per kilobase of

transcript per million fragments mapped (FPKM) were estimated using Cufflinks software (http://cole-trapnell-lab.github.io/cufflinks/) [104].

Identification of AtLBR-2-dependent up- or down-regulated genes. The differential expression between pLPS-treated WT and the three other data sets (untreated WT, pLPS-treated *atlbr-2-1*, and untreated *atlbr-2-1*) were calculated in R packages, edgeR (https://bioconductor.org/packages/release/bioc/html/edgeR.html) [105] and TCC (http://bioconductor.org/packages/release/bioc/html/TCC.html) [106] using the read counts of each data set, which were calculated by HTSeq-count (https://htseq.readthedocs.io/en/release_0.9.1/index.html) [107]. When compared to RNA-Seq data obtained from pLPS-treated WT, genes with negative Log_2FC value changes (FDR; false discovery rate < 0.01, $Log_2FC < -1.35$) were identified as up-regulated genes in pLPS-treated WT. In contrast, genes with positive Log_2FC value changes (FDR < 0.01, $Log_2FC > 1.35$) were identified as down-regulated genes in pLPS-treated WT. Commonly up-regulated or down-regulated genes were investigated and 65 and 2 genes were identified as AtLBR-2-dependent up- and down-regulated genes, respectively.

GO enrichment analysis. The GO enrichment analysis for pLPS-induced up- or down-regulated genes in the WT plants was performed using functional annotation charts of DAVID Bioinformatics Resources 6.7 (https://david-d.ncifcrf.gov/) [108]. The distributions of GO terms at levels 1 or 2 for CC, MF, and BP for the 65 AtLBR-2-dependent up-regulated genes were analyzed using the VirtualPlant 1.3 online tool (http://virtualplant.bio.nyu.edu/cgi-bin/vpweb/) [109].

Pathway analysis. The pathway analysis of the 65 AtLBR-2-dependent up-regulated genes was performed via KOBAS 3.0 (http://kobas.cbi.pku.edu.cn/), which uses the BioCyc (https://biocyc.org/), KEGG (http://www.genome.jp/kegg/), and PANTHER (http://pantherdb.org/) databases [110, 111]. Only pathways with *P*-value < 0.01 were listed.

qRT-PCR analysis. After the pLPS or SA treatment and total RNA isolation, as above, reverse transcription was performed using 1 μg of total RNA [40]. qRT-PCR was run on a PikoReal real-time PCR system (Thermo Fisher Scientific), according to the manufacturer's recommendations using the following conditions: 1 min at 95ºC, and 40 cycles of 5 s at 95ºC and 30 s at 60ºC. Because the FPKM values of *β-tubulin4* (AT5G44340) were not affected by pLPS treatment, it was used as a non-responsive reference gene (Fig. 2-10). The sequences of

gene-specific primers are mentioned in Table 2-9. Each experiment was repeated at least three times.

Free SA and SAG measurement. Two-week-old *Arabidopsis* seedlings grown on MS agar plates were transferred to liquid MS medium and treated with 100 μg/ml pLPS for the indicated time points. After the treatment, 80 mg of whole plants were harvested. Both free SA and SAG extraction was performed, based on a previously-reported method [112, 113]. Free SA and SAG were quantified by reverse-phase HPLC on a C18 column (YMC) and monitored by UV-detection at 240 nm. The column was eluted with 50 to 90% acetonitrile gradient in water containing 0.1% trifluoroacetic acid.

Table 2-8. Mapping results of RNA-Seq reads from pLPS untreated (0 h) and treated (24 h) *Arabidopsis* plants calculated by TopHat software.

Sample		Input	Mapped	Multiple alignments	Mapped percent [%]
WT_0h-1	left		9108355	733630	88.5
	right	10291798	9064807	729268	88.1
	aligned pair		8986163	723249	86.1
WT_0h-2	left		10002374	270397	91.7
	right	10910276	9947049	266488	91.2
	aligned pair		9875713	266488	89.8
WT_0h-3	left		9588682	246155	94.5
	right	10147734	9532742	244181	93.9
	aligned pair		9461137	242512	92.4

WT_24h-1	left		9622012	222224	95.0
	right	10129203	9573317	220570	94.5
	aligned pair		9500722	219105	93.1
WT_24h-2	left		8979667	273784	94.7
	right	9485142	8930638	271879	94.2
	aligned pair		8862851	269952	92.7
WT_24h-3	left		8733723	159468	93.0
	right	9386663	8687862	158361	92.6
	aligned pair		8626426	157141	91.3
*atlbr-2*_0h-1	left		9820040	185958	95.1
	right	10321160	9767160	184238	94.6
	aligned pair		9690135	182947	93.1
*atlbr-2*_0h-2	left		9515306	192782	95.0
	right	10017028	9462903	190974	94.5
	aligned pair		9396537	189689	93.2
*atlbr-2*_0h-3	left		9536469	229329	92.9
	right	10267907	10267907	9474913	92.3
	aligned pair		9474913	227425	91.0
atlbr-2_24h-1	left		10593345	223351	92.8
	right	11418139	11418139	221719	92.3
	aligned pair		10455241	219724	90.7
*atlbr-2*_24h-2	left		11149809	211255	93.3
	right	11953181	11092323	209840	92.8
	aligned pair		11010533	208134	91.5
*atlbr-2*_24h-3	left		10146975	162874	95.4
	right	10639475	10095988	161643	94.9
	aligned pair		10021227	160545	93.5

Table 2-9. Primer sets used in Chapter 2 for qRT-PCR.

Set	F/R	Sequence
CYP71A13	F	5′- CCCTCAGTCTCAGGTACGGA -3′
	R	5′- ACCTCTTGAGCTGCTTCACC -3′
LURP1	F	5′- CAGCCCTGTGTGATAGTGGG -3′
	R	5′- CTTACCGTCCGCACTCGTTA -3′
PNP-A	F	5′- TCGGAGGTACAGGGTTCGAT -3′
	R	5′- GCGATAACCCGAAAAGCGTC -3′
AIG1	F	5′- GCTCGCAGCATTGATGAAGG -3′
	R	5′- CTTCTCCTGCGCCTCCATAG -3′
GSTF7	F	5′- CATGTCAGTGCTTGGGTTGC -3′
	R	5′- TAGGGCAATGAGGTCATCGC -3′
PDR12	F	5′- TTCTTTGCCTTGGGTGGTGT -3′
	R	5′- CTCATTGGCTAGGATCGCGT -3′
PR1	F	5′- GGAGCTACGCAGAACAACTAAGA -3′
	R	5′- CCCACGAGGATCATAGTTGCAACTGA -3′
β-Tubulin4	F	5′- GAGGGAGCCATTGACAACATCTT -3′
	R	5′- GCGAACAGTTCACAGCTATGTTCA -3′
HVA22B	F	5′- TGGTCTTACCGGGCATGAAC -3′
	R	5′- TTGCTCCCAAGTCGTCATCC -3′
PDF1.3	F	5′- GCGAGAAGCCAAGTGGTACT -3′
	R	5′- TGTTTTGCCCCCTCAAGGTT -3′
CLE21	F	5′- ACAAGGTTGTGATCACGGAGA -3′
	R	5′- AAGGATTTGGACCTGTGGGG -3′
HAI2	F	5′- GGTGCAAGAGTCTTAGGCGT -3′
	R	5′- CTCAGTCCGATCCGTAACCG -3′
LEA4-5	F	5′- AAGAGAGAAACGCGTCAGCA -3′
	R	5′- GTCCAGTGGTCGAGTGAGTG -3′
UNE11	F	5′- CCGCCACGTCATCAAAAGAC -3′
	R	5′- TGAACGCACGTAACGAGACA -3′
AT3G20340	F	5′- TCAGGCTCACGAAGAAGCAA -3′
	R	5′- ACCCGCGATTGTTCAGGATT -3′
HR2	F	5′- CCACTGATGGCTAAGGTCGA -3′
	R	5′- CGTTTGAGCTCCGCATAAGC -3′
ATH2	F	5′- TCTCCTTCTGCTACCGGTGA -3′

	R	5′- GACCATCTCCTAGGCCATGC -3′
MES13	F	5′- ACCAGCTCGTTGACAAGGAG -3′
	R	5′- GTACCAACACCAAGCTCCGA -3′
M17	F	5′- TGCCACACACGATGAAGTGA -3′
	R	5′- TTGCTGGGGCTCTACAACAG -3′
PR12	F	5′- TGGTGGAAGCACAGAAGTTGT -3′
	R	5′- CACTGATTCTTGCACGCGTT -3′
PP2-A6	F	5′- GGGTGGATATTTTGGCCGGA -3′
	R	5′- TCGTGGGACGTATTGCAACA -3′
PROPEP3	F	5′- CGTCATCACACAGCGAGGAA -3′
	R	5′- TCCTTTTCCTGAACTTGGCGT -3′

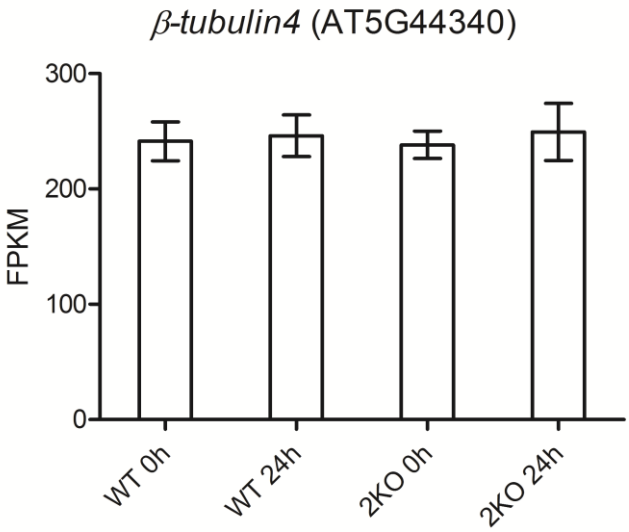

Figure 2-10. The FPKM values of *β-tubulin4* (AT5G44340) between samples.

The FPKM values of *β-tubulin4* were estimated by Cufflinks software. Mean FPKM values were calculated from the results of three biological replicates. Means ± standard errors are presented. Significant differences among means compared each other were evaluated by one-way ANOVA followed by Tukey's multiple comparison test.

Concluding remarks

Here, I characterised two genes of *Arabidopsis*, *AtLBR-1* and *AtLBR-2*, which belong to the LBP/BPI subfamily rather than the PLUNC subfamily. My results showed that the recombinant N-terminal domain of AtLBRs is found to bind to LPS directly, and that LPS-treated *atlbr* mutants showed the defect in immune responses, such as *PR1* gene expression and ROS production. My study is the first to reveal the biological importance of LBRs for induction of LPS-triggered defence responses in plants and the functional similarities among LBP/BPI subfamily from various organisms. Furthermore, I have studied here the analysis of the genome-wide effect of AtLBR-2 on pLPS-induced gene expression. The transcriptome analyses performed in this study identify the 65 AtLBR-2-dependent up-regulated genes, and reveal an indispensable key role of AtLBR-2 in the up-regulation of defense-related genes and in the LPS-induced SA signaling pathway. Altogether, my results reveal the importance of AtLBRs in LPS recognition and signaling mechanisms in plants. My study provide increased understanding of the details of plant innate immunity mechanisms against pathogens containing LPS.

References

1. Zeidler D, Zähringer U, Gerber I, Dubery I, Hartung T, Bors W, et al. Innate immunity in Arabidopsis thaliana: Lipopolysaccharides activate nitric oxide synthase (NOS) and induce defense genes. Proc Natl Acad Sci. 2004;101:15811–15816.

2. Desaki Y, Miya A, Venkatesh B, Tsuyumu S, Yamane H, Kaku H, et al. Bacterial lipopolysaccharides induce defense responses associated with programmed cell death in rice cells. Plant Cell Physiol. 2006;47:1530–1540.

3. Melotto M, Underwood W, Koczan J, Nomura K, He SY. Plant stomata function in innate immunity against bacterial invasion. Cell. 2006;126:969–980.

4. Ranf S, Gisch N, Schäffer M, Illig T, Westphal L, Knirel YA, et al. A lectin S-domain receptor kinase mediates lipopolysaccharide sensing in Arabidopsis thaliana. Nat Immunol. 2015;16:426–433.

5. Weiss J. Bactericidal/permeability-increasing protein (BPI) and lipopolysaccharide-binding protein (LBP): structure, function and regulation in host defence against Gram-negative bacteria. Biochem Soc Trans. 2003;31:785–790.

6. Vesy CJ, Kitchens RL, Wolfbauer G, Albers JJ, Munford RS. Lipopolysaccharide-Binding Protein and Phospholipid Transfer Protein Release Lipopolysaccharides from Gram-Negative Bacterial Membranes. Infect Immun. 2000;68:2410–2417.

7. Bingle CD, LeClair EE, Havard S, Bingle L, Gillingham P, Craven CJ. Phylogenetic and evolutionary analysis of the PLUNC gene family. Protein Sci Publ Protein Soc. 2004;13:422–430.

8. Ghafouri B, Kihlström E, Tagesson C, Lindahl M. PLUNC in human nasal lavage fluid: multiple isoforms that bind to lipopolysaccharide. Biochim Biophys Acta. 2004;1699:57–63.

9. Geetha C, Venkatesh SG, Dunn BHF, Gorr S-U. Expression and anti-bacterial activity of human parotid secretory protein (PSP). Biochem Soc Trans. 2003;31:815–818.

10. Gautron J, Murayama E, Vignal A, Morisson M, McKee MD, Réhault S, et al. Cloning of Ovocalyxin-36, a Novel Chicken Eggshell Protein Related to Lipopolysaccharide-binding Proteins, Bactericidal Permeability-increasing Proteins, and Plunc Family Proteins. J Biol Chem. 2007;282:5273–5286.

11. Inagawa H, Honda T, Kohchi C, Nishizawa T, Yoshiura Y, Nakanishi T, et al. Cloning and Characterization of the Homolog of Mammalian Lipopolysaccharide-Binding Protein and Bactericidal Permeability-Increasing Protein in Rainbow Trout Oncorhynchus mykiss. J Immunol. 2002;168:5638–5644.

12. Stenvik J, Solstad T, Strand C, Leiros I, Jørgensen TØ. Cloning and analyses of a BPI/LBP cDNA of the Atlantic cod (Gadus morhua L.). Dev Comp Immunol. 2004;28:307–323.

13. Kono T, Sakai M. Molecular cloning of a novel bactericidal permeability-increasing protein/lipopolysaccharide-binding protein (BPI/LBP) from common carp Cyprinus carpio L. and its expression. Mol Immunol. 2003;40:269–278.

14. Suzuki K, Izumi S, Tanaka H, Katagiri T. Molecular cloning and expression analysis of the BPI/LBP cDNA and its gene from ayu Plecoglossus altivelis altivelis. Fish Sci. 2009;75:673–681.

15. Gonzalez M, Gueguen Y, Destoumieux-Garzón D, Romestand B, Fievet J, Pugnière M, et al. Evidence of a bactericidal permeability increasing protein in an invertebrate, the Crassostrea gigas Cg-BPI. Proc Natl Acad Sci. 2007;104:17759–11764.

16. Cordeiro CMM, Esmaili H, Ansah G, Hincke MT. Ovocalyxin-36 Is a Pattern Recognition Protein in Chicken Eggshell Membranes. PLOS ONE. 2013;8:e84112.

17. Zhang Y, He X, Li X, Fu D, Chen J, Yu Z. The second bactericidal permeability increasing protein (BPI) and its revelation of the gene duplication in the Pacific oyster, Crassostrea gigas. Fish Shellfish Immunol. 2011;30:954–963.

18. Beamer LJ, Carroll SF, Eisenberg D. Crystal Structure of Human BPI and Two Bound Phospholipids at 2.4 Angstrom Resolution. Science. 1997;276:1861–1864.

19. Kohara J, Tsuneyoshi N, Gauchat J-F, Kimoto M, Fukudome K. Preparation and characterization of truncated human lipopolysaccharide-binding protein in Escherichia coli. Protein Expr Purif. 2006;49:276–283.

20. Walker TS, Bais HP, Déziel E, Schweizer HP, Rahme LG, Fall R, et al. Pseudomonas aeruginosa-Plant Root Interactions. Pathogenicity, Biofilm Formation, and Root Exudation. Plant Physiol. 2004;134:320–331.

21. Rahme LG, Stevens EJ, Wolfort SF, Shao J, Tompkins RG, Ausubel FM. Common

virulence factors for bacterial pathogenicity in plants and animals. Science. 1995;268:1899–1902.

22. Capodici C, Chen S, Sidorczyk Z, Elsbach P, Weiss J. Effect of lipopolysaccharide (LPS) chain length on interactions of bactericidal/permeability-increasing protein and its bioactive 23-kilodalton NH_2-terminal fragment with isolated LPS and intact Proteus mirabilis and Escherichia coli. Infect Immun. 1994;62:259–265.

23. Gazzano-Santoro H, Parent JB, Grinna L, Horwitz A, Parsons T, Theofan G, et al. High-affinity binding of the bactericidal/permeability-increasing protein and a recombinant amino-terminal fragment to the lipid A region of lipopolysaccharide. Infect Immun. 1992;60:4754–4761.

24. Faulkner C, Robatzek S. Plants and pathogens: putting infection strategies and defence mechanisms on the map. Curr Opin Plant Biol. 2012;15:699–707.

25. Erbs G, Jensen TT, Silipo A, Grant W, Dow JM, Molinaro A, et al. An antagonist of lipid A action in mammals has complex effects on lipid A induction of defence responses in the model plant Arabidopsis thaliana. Microbes Infect. 2008;10:571–574.

26. Bedini E, De Castro C, Erbs G, Mangoni L, Dow JM, Newman M-A, et al. Structure-Dependent Modulation of a Pathogen Response in Plants by Synthetic O-Antigen Polysaccharides. J Am Chem Soc. 2005;127:2414–2416.

27. Huuskonen J, Olkkonen VM, Jauhiainen M, Ehnholm C. The impact of phospholipid transfer protein (PLTP) on HDL metabolism. Atherosclerosis. 2001;155:269–281.

28. Hall J, Qiu X. Structural and biophysical insight into cholesteryl ester-transfer protein. Biochem Soc Trans. 2011;39:1000–1005.

29. Hailman E, Albers JJ, Wolfbauer G, Tu A-Y, Wright SD. Neutralization and Transfer of Lipopolysaccharide by Phospholipid Transfer Protein. J Biol Chem. 1996;271:12172–12178.

30. Eckert JK, Kim YJ, Kim JI, Gürtler K, Oh D-Y, Sur S, et al. The Crystal Structure of Lipopolysaccharide Binding Protein Reveals the Location of a Frequent Mutation that Impairs Innate Immunity. Immunity. 2013;39:647–660.

31. Qiu X, Mistry A, Ammirati MJ, Chrunyk BA, Clark RW, Cong Y, et al. Crystal structure of cholesteryl ester transfer protein reveals a long tunnel and four bound lipid molecules. Nat Struct Mol Biol. 2007;14:106–113.

32. Shah J. The salicylic acid loop in plant defense. Curr Opin Plant Biol. 2003;6:365–371.

33. Ishikawa K, Yoshimura K, Harada K, Fukusaki E, Ogawa T, Tamoi M, et al. AtNUDX6, an ADP-Ribose/NADH Pyrophosphohydrolase in Arabidopsis, Positively Regulates NPR1-Dependent Salicylic Acid Signaling. Plant Physiol. 2010;152:2000–2012.

34. Herrera-Vásquez A, Salinas P, Holuigue L. Salicylic acid and reactive oxygen species interplay in the transcriptional control of defense genes expression. Front Plant Sci. 2015;6: 171.

35. Iizasa E, Nagano Y. Highly efficient yeast-based in vivo DNA cloning of multiple DNA fragments and the simultaneous construction of yeast/Escherichia coli shuttle vectors. BioTechniques. 2006;40:79–83.

36. Fujii Y, Kodama Y. In planta comparative analysis of improved green fluorescent proteins with reference to fluorescence intensity and bimolecular fluorescence complementation ability. Plant Biotechnol. 2015;32:81–87.

37. Nagano Y, Takao S, Kudo T, Iizasa E, Anai T. Yeast-based recombineering of DNA fragments into plant transformation vectors by one-step transformation. Plant Cell Rep. 2007;26:2111–2117.

38. Journot-Catalino N, Somssich IE, Roby D, Kroj T. The Transcription Factors WRKY11 and WRKY17 Act as Negative Regulators of Basal Resistance in Arabidopsis thaliana. Plant Cell. 2006;18:3289–3302.

39. Kunze G, Zipfel C, Robatzek S, Niehaus K, Boller T, Felix G. The N Terminus of Bacterial Elongation Factor Tu Elicits Innate Immunity in Arabidopsis Plants. Plant Cell. 2004;16:3496–3507.

40. Iizasa S, Iizasa E, Matsuzaki S, Tanaka H, Kodama Y, Watanabe K, et al. Arabidopsis LBP/BPI related-1 and -2 bind to LPS directly and regulate PR1 expression. Sci Rep. 2016;6:27527.

41. Madala NE, Molinaro A, Dubery IA. Distinct carbohydrate and lipid-based molecular patterns within lipopolysaccharides from Burkholderia cepacia contribute to defense-associated differential gene expression in Arabidopsis thaliana. Innate Immun. 2012;18:140–154.

42. Uknes S, Mauch-Mani B, Moyer M, Potter S, Williams S, Dincher S, et al. Acquired

resistance in Arabidopsis. Plant Cell. 1992;4:645–656.

43. Bricchi I, Bertea CM, Occhipinti A, Paponov IA, Maffei ME. Dynamics of membrane potential variation and gene expression induced by Spodoptera littoralis, Myzus persicae, and Pseudomonas syringae in Arabidopsis. PLOS ONE. 2012;7:e46673.

44. Schuhegger R, Nafisi M, Mansourova M, Petersen BL, Olsen CE, Svatoš A, et al. CYP71B15 (PAD3) catalyzes the final step in camalexin biosynthesis. Plant Physiol. 2006;141:1248–1254.

45. Morán-Diez E, Rubio B, Domínguez S, Hermosa R, Monte E, Nicolás C. Transcriptomic response of Arabidopsis thaliana after 24h incubation with the biocontrol fungus Trichoderma harzianum. J Plant Physiol. 2012;169:614–620.

46. Borges AA, Dobon A, Expósito-Rodríguez M, Jiménez-Arias D, Borges-Pérez A, Casañas-Sánchez V, et al. Molecular analysis of menadione-induced resistance against biotic stress in Arabidopsis. Plant Biotechnol J. 2009;7:744–762.

47. Loon LC van, Rep M, Pieterse CMJ. Significance of inducible defense-related rroteins in infected plants. Annu Rev Phytopathol. 2006;44:135–162.

48. Kus JV, Zaton K, Sarkar R, Cameron RK. Age-related resistance in Arabidopsis is a developmentally regulated defense response to Pseudomonas syringae. Plant Cell Online. 2002;14:479–490.

49. Bourdais G, Burdiak P, Gauthier A, Nitsch L, Salojärvi J, Rayapuram C, et al. Large-scale phenomics identifies primary and fine-tuning roles for CRKs in responses related to oxidative stress. PLOS Genet. 2015;11:e1005373.

50. Blanco F, Salinas P, Cecchini NM, Jordana X, Hummelen PV, Alvarez ME, et al. Early genomic responses to salicylic acid in Arabidopsis. Plant Mol Biol. 2009;70:79–102.

51. Breitenbach HH, Wenig M, Wittek F, Jordá L, Maldonado-Alconada AM, Sarioglu H, et al. Contrasting roles of the apoplastic aspartyl protease APOPLASTIC, ENHANCED DISEASE SUSCEPTIBILITY1-DEPENDENT1 and LEGUME LECTIN-LIKE PROTEIN1 in Arabidopsis systemic acquired resistance. Plant Physiol. 2014;165:791–809.

52. Jakab G, Manrique A, Zimmerli L, Métraux J-P, Mauch-Mani B. Molecular characterization of a novel lipase-like pathogen-inducible gene family of Arabidopsis. Plant Physiol. 2003;132:2230–2239.

53. Jung HW, Tschaplinski TJ, Wang L, Glazebrook J, Greenberg JT. Priming in systemic plant immunity. Science. 2009;324:89–91.

54. Reuber TL, Ausubel FM. Isolation of Arabidopsis genes that differentiate between resistance responses mediated by the RPS2 and RPM1 disease resistance genes. Plant Cell Online. 1996;8:241–249.

55. Mészáros T, Helfer A, Hatzimasoura E, Magyar Z, Serazetdinova L, Rios G, et al. The Arabidopsis MAP kinase kinase MKK1 participates in defence responses to the bacterial elicitor flagellin. Plant J. 2006;48:485–498.

56. Denoux C, Galletti R, Mammarella N, Gopalan S, Werck D, De Lorenzo G, et al. Activation of defense response pathways by OGs and Flg22 elicitors in Arabidopsis seedlings. Mol Plant. 2008;1:423–445.

57. Du Z, Xu D, Li L, Shi Y, Schläppi M, Xu Z-Q. Inhibitory effects of Arabidopsis EARLI1 against Botrytis cinerea and Bradysia difformis. Plant Cell Tissue Organ Cult PCTOC. 2012;110:435–443.

58. Karim S, Holmström K-O, Mandal A, Dahl P, Hohmann S, Brader G, et al. AtPTR3, a wound-induced peptide transporter needed for defence against virulent bacterial pathogens in Arabidopsis. Planta. 2006;225:1431–1445.

59. Hok S, Danchin EGJ, Allasia V, Panabières F, Attard A, Keller H. An Arabidopsis (malectin-like) leucine-rich repeat receptor-like kinase contributes to downy mildew disease. Plant Cell Environ. 2011;34:1944–1957.

60. Asano T, Kimura M, Nishiuchi T. The defense response in Arabidopsis thaliana against Fusarium sporotrichioides. Proteome Sci. 2012;10:61.

61. Frey NF dit, Mbengue M, Kwaaitaal M, Nitsch L, Altenbach D, Häweker H, et al. Plasma membrane calcium ATPases are important components of receptor-mediated signaling in plant immune responses and development. Plant Physiol. 2012;159:798–809.

62. Chen K, Fan B, Du L, Chen Z. Activation of hypersensitive cell death by pathogen-induced receptor-like protein kinases from Arabidopsis. Plant Mol Biol. 2004;56:271–283.

63. Quirino BF, Normanly J, Amasino RM. Diverse range of gene activity during Arabidopsis thaliana leaf senescence includes pathogen-independent induction of

defense-related genes. Plant Mol Biol. 1999;40:267–278.

64. Yi SY, Shirasu K, Moon JS, Lee S-G, Kwon S-Y. The activated SA and JA signaling pathways have an influence on flg22-triggered oxidative burst and callose deposition. PLOS ONE. 2014;9:e88951.

65. Gruner K, Griebel T, Návarová H, Attaran E, Zeier J. Reprogramming of plants during systemic acquired resistance. Front Plant Sci. 2013;4:252:1

66. Lieberherr D, Wagner U, Dubuis P-H, Métraux J-P, Mauch F. The rapid Induction of glutathione S-transferases AtGSTF2 and AtGSTF6 by avirulent Pseudomonas syringae is the result of combined salicylic acid and ethylene signaling. Plant Cell Physiol. 2003;44:750–757.

67. Tsuda K, Sato M, Glazebrook J, Cohen JD, Katagiri F. Interplay between MAMP-triggered and SA-mediated defense responses. Plant J. 2008;53:763–775.

68. Blanco F, Garretón V, Frey N, Dominguez C, Pérez-Acle T, Straeten DV der, et al. Identification of NPR1-dependent and independent genes early induced by salicylic acid treatment in Arabidopsis. Plant Mol Biol. 2005;59:927–944.

69. Siemens J, Keller I, Sarx J, Kunz S, Schuller A, Nagel W, et al. Transcriptome analysis of Arabidopsis clubroots indicate a key role for cytokinins in disease development. Mol Plant Microbe Interact. 2006;19:480–494.

70. Gechev TS, Gadjev IZ, Hille J. An extensive microarray analysis of AAL-toxin-induced cell death in Arabidopsis thaliana brings new insights into the complexity of programmed cell death in plants. Cell Mol Life Sci CMLS. 2004;61:1185–1197.

71. Bethke G, Grundman RE, Sreekanta S, Truman W, Katagiri F, Glazebrook J. Arabidopsis PECTIN METHYLESTERASEs contribute to immunity against Pseudomonas syringae. Plant Physiol. 2014;164:1093–1107.

72. Nafisi M, Goregaoker S, Botanga CJ, Glawischnig E, Olsen CE, Halkier BA, et al. Arabidopsis cytochrome P450 monooxygenase 71A13 catalyzes the conversion of indole-3-acetaldoxime in camalexin synthesis. Plant Cell. 2007;19:2039–2052.

73. Ferrari S, Galletti R, Denoux C, Lorenzo GD, Ausubel FM, Dewdney J. Resistance to Botrytis cinerea induced in Arabidopsis by elicitors is independent of salicylic acid, ethylene, or jasmonate signaling but requires PHYTOALEXIN DEFICIENT3. Plant Physiol.

2007;144:367–379.

74. Campbell EJ, Schenk PM, Kazan K, Penninckx IAMA, Anderson JP, Maclean DJ, et al. Pathogen-responsive expression of a putative ATP-binding cassette transporter gene conferring resistance to the diterpenoid sclareol is regulated by multiple defense signaling pathways in Arabidopsis. Plant Physiol. 2003;133:1272–1284.

75. Chen L, Zhang L, Yu D. Wounding-induced WRKY8 is involved in basal defense in Arabidopsis. Mol Plant Microbe Interact. 2010;23:558–565.

76. Nobuta K, Okrent RA, Stoutemyer M, Rodibaugh N, Kempema L, Wildermuth MC, et al. The GH3 acyl adenylase family member PBS3 regulates salicylic acid-dependent defense responses in Arabidopsis. Plant Physiol. 2007;144:1144–1156.

77. Acharya BR, Raina S, Maqbool SB, Jagadeeswaran G, Mosher SL, Appel HM, et al. Overexpression of CRK13, an Arabidopsis cysteine-rich receptor-like kinase, results in enhanced resistance to Pseudomonas syringae. Plant J. 2007;50:488–499.

78. Trost G, Vi SL, Czesnick H, Lange P, Holton N, Giavalisco P, et al. Arabidopsis poly(A) polymerase PAPS1 limits founder-cell recruitment to organ primordia and suppresses the salicylic acid-independent immune response downstream of EDS1/PAD4. Plant J. 2014;77:688–699.

79. Ishihama N, Yoshioka H. Post-translational regulation of WRKY transcription factors in plant immunity. Curr Opin Plant Biol. 2012;15:431–437.

80. Fu ZQ, Yan S, Saleh A, Wang W, Ruble J, Oka N, et al. NPR3 and NPR4 are receptors for the immune signal salicylic acid in plants. Nature. 2012;486:228–232.

81. Noutoshi Y, Kuromori T, Wada T, Hirayama T, Kamiya A, Imura Y, et al. Loss of NECROTIC SPOTTED LESIONS 1 associates with cell death and defense responses in Arabidopsis thaliana. Plant Mol Biol. 2006;62:29–42.

82. Tutsui T, Morita-Yamamuro C, Asada Y, Minami E, Shibuya N, Ikeda A, et al. Salicylic acid and a chitin elicitor both control expression of the CAD1 gene involved in the plant immunity of Arabidopsis. Biosci Biotechnol Biochem. 2006;70:2042–2048.

83. Seo PJ, Park C-M. MYB96-mediated abscisic acid signals induce pathogen resistance response by promoting salicylic acid biosynthesis in Arabidopsis. New Phytol. 2010;186:471–483.

84. McDowell JM, Cuzick A, Can C, Beynon J, Dangl JL, Holub EB. Downy mildew (Peronospora parasitica) resistance genes in Arabidopsis vary in functional requirements for NDR1, EDS1, NPR1 and salicylic acid accumulation. Plant J. 2000;22:523–529.

85. Schön M, Töller A, Diezel C, Roth C, Westphal L, Wiermer M, et al. Analyses of wrky18 wrky40 plants reveal critical roles of SA/EDS1 signaling and indole-glucosinolate biosynthesis for golovinomyces orontii resistance and a loss-of resistance towards Pseudomonas syringae pv. tomato AvrRPS4. Mol Plant Microbe Interact. 2013;26:758–767.

86. Suzuki N, Bajad S, Shuman J, Shulaev V, Mittler R. The transcriptional co-activator MBF1c is a key regulator of thermotolerance in Arabidopsis thaliana. J Biol Chem. 2008;283:9269–9275.

87. Murray SL, Ingle RA, Petersen LN, Denby KJ. Basal resistance against Pseudomonas syringae in Arabidopsis involves WRKY53 and a protein with homology to a nematode resistance protein. Mol Plant Microbe Interact. 2007;20:1431–1438.

88. Zeidler D, Dubery IA, Schmitt-Kopplin P, Von Rad U, Durner J. Lipopolysaccharide mobility in leaf tissue of Arabidopsis thaliana. Mol Plant Pathol. 2010;11:747–755.

89. Lim CW, Luan S, Lee SC. A prominent role for RCAR3-mediated ABA signaling in response to Pseudomonas syringae pv. tomato DC3000 infection in Arabidopsis. Plant Cell Physiol. 2014;55:10:1691–1703.

90. Datta R, Sinha R, Chattopadhyay S. Changes in leaf proteome profile of Arabidopsis thaliana in response to salicylic acid. J Biosci. 2013;38:317–328.

91. Beets CA, Huang J-C, Madala NE, Dubery I. Activation of camalexin biosynthesis in Arabidopsis thaliana in response to perception of bacterial lipopolysaccharides: a gene-to-metabolite study. Planta. 2012;236:261–272.

92. Zhao J, Last RL. Coordinate regulation of the tryptophan biosynthetic pathway and indolic phytoalexin accumulation in Arabidopsis. Plant Cell. 1996;8:2235–2244.

93. Glazebrook J, Rogers EE, Ausubel FM. Isolation of Arabidopsis mutants with enhanced disease susceptibility by direct screening. Genetics. 1996;143:973–982.

94. Mosher RA, Durrant WE, Wang D, Song J, Dong X. A comprehensive structure–function analysis of Arabidopsis SNI1 defines essential regions and transcriptional repressor activity. Plant Cell. 2006;18:1750–1765.

95. Kim C, Meskauskiene R, Zhang S, Lee KP, Ashok ML, Blajecka K, et al. Chloroplasts of Arabidopsis are the source and a primary target of a plant-specific programmed cell death signaling pathway. Plant Cell. 2012;24:3026–3039.

96. Šimková K, Moreau F, Pawlak P, Vriet C, Baruah A, Alexandre C, et al. Integration of stress-related and reactive oxygen species-mediated signals by Topoisomerase VI in Arabidopsis thaliana. Proc Natl Acad Sci. 2012;109:16360–16365.

97. Triantaphylidès C, Havaux M. Singlet oxygen in plants: production, detoxification and signaling. Trends Plant Sci. 2009;14:219–228.

98. Elmore JM, Coaker G. The role of the plasma membrane H^+-ATPase in plant–microbe interactions. Mol Plant. 2011;4:416–427.

99. Segonzac C, Zipfel C. Activation of plant pattern-recognition receptors by bacteria. Curr Opin Microbiol. 2011;14:54–61.

100. Zipfel C, Kunze G, Chinchilla D, Caniard A, Jones JDG, Boller T, et al. Perception of the bacterial PAMP EF-Tu by the receptor EFR restricts Agrobacterium-mediated transformation. Cell. 2006;125:749–760.

101. Vaid N, Pandey PK, Tuteja N. Genome-wide analysis of lectin receptor-like kinase family from Arabidopsis and rice. Plant Mol Biol. 2012;80:365–388.

102. Sanabria NM, van Heerden H, Dubery IA. Molecular characterisation and regulation of a Nicotiana tabacum S-domain receptor-like kinase gene induced during an early rapid response to lipopolysaccharides. Gene. 2012;501:39–48.

103. Chen F, D'Auria JC, Tholl D, Ross JR, Gershenzon J, Noel JP, et al. An Arabidopsis thaliana gene for methylsalicylate biosynthesis, identified by a biochemical genomics approach, has a role in defense. Plant J. 2003;36:577–588.

104. Trapnell C, Roberts A, Goff L, Pertea G, Kim D, Kelley DR, et al. Differential gene and transcript expression analysis of RNA-seq experiments with TopHat and Cufflinks. Nat Protoc. 2012;7:562–578.

105. Robinson MD, McCarthy DJ, Smyth GK. edgeR: a Bioconductor package for differential expression analysis of digital gene expression data. Bioinformatics. 2010;26:139–140.

106. Sun J, Nishiyama T, Shimizu K, Kadota K. TCC: an R package for comparing tag count

data with robust normalization strategies. BMC Bioinformatics. 2013;14:219.

107. Anders S, Pyl PT, Huber W. HTSeq—a Python framework to work with high-throughput sequencing data. Bioinformatics. 2015;31:166–169.

108. Huang DW, Sherman BT, Lempicki RA. Systematic and integrative analysis of large gene lists using DAVID bioinformatics resources. Nat Protoc. 2008;4:44–57.

109. Katari MS, Nowicki SD, Aceituno FF, Nero D, Kelfer J, Thompson LP, et al. VirtualPlant: A software platform to support systems biology research. Plant Physiol. 2010;152:500–515.

110. Xie C, Mao X, Huang J, Ding Y, Wu J, Dong S, et al. KOBAS 2.0: a web server for annotation and identification of enriched pathways and diseases. Nucleic Acids Res. 2011;39 suppl 2:W316–322.

111. Wu J, Mao X, Cai T, Luo J, Wei L. KOBAS server: a web-based platform for automated annotation and pathway identification. Nucleic Acids Res. 2006;34 suppl 2:W720–724.

112. Li X, Zhang Y, Clarke JD, Li Y, Dong X. Identification and cloning of a negative regulator of systemic acquired resistance, SNI1, through a screen for suppressors of npr1-1. Cell. 1999;98:329–339.

113. Bowling SA, Guo A, Cao H, Gordon AS, Klessig DF, Dong X. A mutation in Arabidopsis that leads to constitutive expression of systemic acquired resistance. Plant Cell. 1994;6:1845–1857.